Sample preparation and assay for lipase activity

For the preparation of total cell extracts, transfected COS7 cells were collected, washed three times with PBS, and disrupted by sonication in a buffer [0.25 M sucrose, 1 mM EDTA (pH 7.0)] containing protease inhibitor cocktails (Sigma). After centrifugation at 15,000 rpm at 4 C for 5 min, supernatants were used for the experiments. Lipase activities of various recombinant ATGL proteins with or without the CGI-58 expressing extract (100 μg protein) were determined by the methods described by Lass *et al.* (12) or Lehner and Verger (17). LD-associated lipase activities in transfected COS7 cells were determined by the method described by Fischer *et al.* (15).

Western blotting analysis

Samples were separated in 5–15% SDS-PAGE gels (Bio-Rad, Tokyo, Japan). Proteins were transferred to 0.2 μm polyvinyl difluoride membranes (Bio-Rad) in Tris/glycine buffer and the membranes probed with anti-ATGL antibody (Cell Signaling Technology, Beverly, MA) at a dilution of 1:1000 or Anti-Xpress antibody (Invitrogen) at a dilution of 1:5000. A secondary antibody (mouse antirabbit IgG-horseradish peroxidase; Amersham Biosciences, Piscataway, NJ) was used at a dilution of 1:5000. Signals were detected by a chemiluminescent reaction (ECL Plus; Amersham Biosciences).

Isolation and immunostaining of peripheral blood leukocytes

Peripheral blood leukocytes were obtained by Ficoll-Hypaque gradient centrifugation (18). Recovered leukocytes were washed in Hank's balanced salt solution and adjusted to a final concentration of 1×10^6/ml for each cytospin preparation; 150,000 cells were distributed on each slide. Slides were then cytocentrifuged at 800 rpm for 10 min with a Shandon centrifuge (Shandon Inc., Pittsburgh, PA), air dried for 30 min, and fixed in cold acetone. In sample sections, endogenous peroxidase was inactivated with 3% hydrogen peroxide in methanol and nonspecific sites inactivated with 0.1% NaN_3 and 1% BSA (Sigma) in PBS. Samples were incubated at room temperature for 1 h with anti-ATGL antibody (Cell Signaling Technology). Immunoreactivity was visualized with 3, 3′-diaminobenzidine tetrahydrochloride using Histofine Simplestain MAX-PO(R) (Nichirei Ltd., Tokyo, Japan) and the samples counterstained with hematoxylin.

Euglycemic-hyperinsulinemic clamp

The insulin-stimulated rate of glucose turnover was assessed as a glucose infusion rate with the infusion of 1.25 mU/kg·min of human insulin (Novo Nordisk, Tokyo, Japan) using an STG 22 artificial pancreas model (Nikkiso Co., Tokyo, Japan) (19). Blood glucose levels were determined every 5 min during the study, and euglycemia (5.5 mM) was maintained by infusion of 20% glucose.

Statistical analysis

Values are presented as mean ± SEM. Results were analyzed with Statview Ver. 5 (SAS Institute Inc., Cary, NC) using one-way ANOVA followed by comparisons using Tukey-Kramer's method. $P < 0.05$ denoted the presence of a statistically significant difference.

Results

Case reports

A 63-yr-old female patient was the seventh child of consanguineous parents. From aged 36 yr, she became aware of muscle weakness and easy fatigability. At age 42 yr, she and her brother were diagnosed with NLSD. Her brother was frequently hospitalized with heart failure, dying of ventricular tachycardia at age 59 yr. At this time she was hospitalized for shortness of breath. She was 149 cm tall and weighed 50.3kg (body mass index 22.7 kg/m^2). Physical examination revealed no ichthyosis, mild hepatomegaly, and mild generalized hypotonia. Laboratory investigations showed vacuolated leukocytes, elevated serum levels of aspartate aminotransferase (322 IU/liter), alanine aminotransferase (177 IU/liter), lactate dehydrogenase (1309 IU/liter), γ-glutamyl transpeptidase (240 IU/liter), and creatinine kinase (742 U/liter). Her plasma myoglobin (170 ng/ml) and aldolase (20.2 IU/liter, 37 C) were elevated. Serum levels of lactate, pyruvate, serum carnitine fraction, and long-chain fatty acid profile were within normal ranges. Serum thyroid stimulating hormone was elevated (8.50 μU/ml), and a heterogeneous echo pattern was detected in the thyroid gland. Fasting plasma glucose was 117 mg/dl and glycated hemoglobin A_{1c} 7.6%. Impaired insulin secretion and normal insulin resistance were suggested by oral glucose loading test (insulinogenic index: (insulin 30 min − insulin 0 min)/(glucose 30 min − glucose 0 min) = 0.23 < 0.4) and hyperinsulinemic-euglycemic clamp study [glucose infusion rate 5 mg/kg·min at insulin infusion rate 1.25 mU/kg·min; normal 4.83 ± 1.70 mg/kg·min (19)]. Urine C-peptide excretion was 69.6 μg/d. Mild fatty liver was suggested from ultrasonography and computed tomography images. Endoscopic ultrasonography showed an atrophic pancreas with heterogeneous parenchyma and no dilatation of the main duct. Brain natriuretic peptide level was markedly elevated (2891 pg/ml). Chest x-ray revealed mild cardiomegaly. Echocardiography showed left ventricular hypertrophy and low diastolic function. Her clinical course is shown in Supplement Fig. 1A, published as supplemental data on The Endocrine Society's Journals Online Web site at http://jcem.endojournals.org. Insulin secretory capacity was assessed as ΔCPR (the increase of serum CPR for 5 min after 1 mg of glucagon iv injection). ΔCPR markedly decreased with age whereas homeostasis model assessment for insulin resistance, an insulin resistance index, stayed almost constant throughout her course.

Optical microscope images of biopsy and autopsy samples and cultured fibroblasts

Biopsy specimens from the liver (Fig. 1, A and B) and muscle (Fig. 1, C and D) of the patient showed marked triglyceride droplets. Autopsy samples of the patient's brother also showed LDs in cardiac muscle (supplemental Fig. 1B), an atrioventricular node (supplemental Fig. 1C), pancreatic acinar cells (supplemental Fig. 1D) and islet cells (supplemental Fig. 1E), renal tubular epithelium, glomerulus (supplemental Fig. 1F), and thyroid gland (supplemental Fig. 1G). Fibroblasts from the patient grew and presented LDs in DMEM with 10% fetal bovine serum. Addition of oleic acid (300 μM) caused more and larger LDs in the cells, compared with control fibroblasts (Fig. 1E).

Detection of ATGL mutation in both alleles of the ATGL gene

The direct sequence of ATGL cDNA revealed that the patient was a homozygote for a 4-bp deletion (799–802delGCCC) (Fig. 2A), leading to a premature stop codon at amino acid position 318, which caused a lack of a C terminus of the protein including the hydrophobic domain (Fig. 2B). This deletion (underlined)

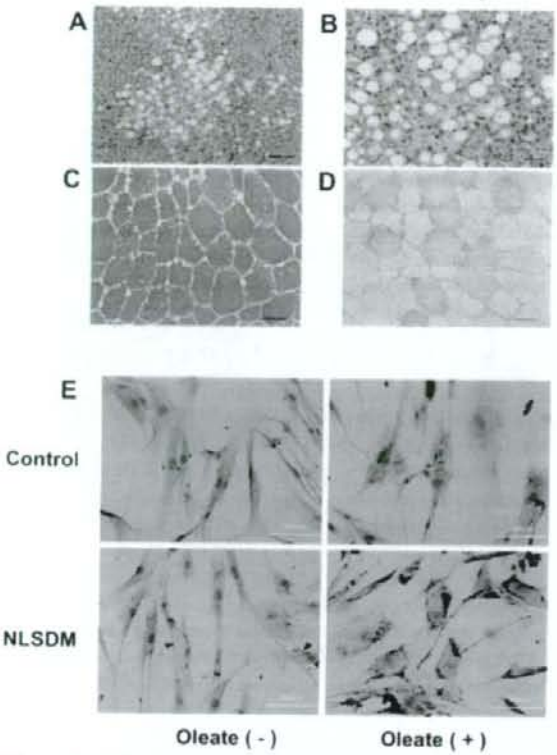

FIG. 1. Light microscopy of formalin-fixed sections of biopsy samples from an individual with NLSDM. Biopsy samples from the patient (A–D) show typical cytosolic lipid deposition. A case report of the patient is described in *Results*. A, Liver; hematoxylin and eosin (H&E), *bar*, 100 μm. B, Liver; H&E, *bar*, 50 μm. C, Muscle; H&E, *bar*, 50 μm. D, Muscle; Sudan, *bar*, 50 μm. E, Fibroblasts obtained from control and an individual with NLSDM were cultured in DMEM (400 mg/dl of glucose) with 10% fetal bovine serum in the presence and absence of 300 μM oleate complexed to BSA. Oil red O staining was performed as described in *Patients and Methods*. *Bar*, 100 μm.

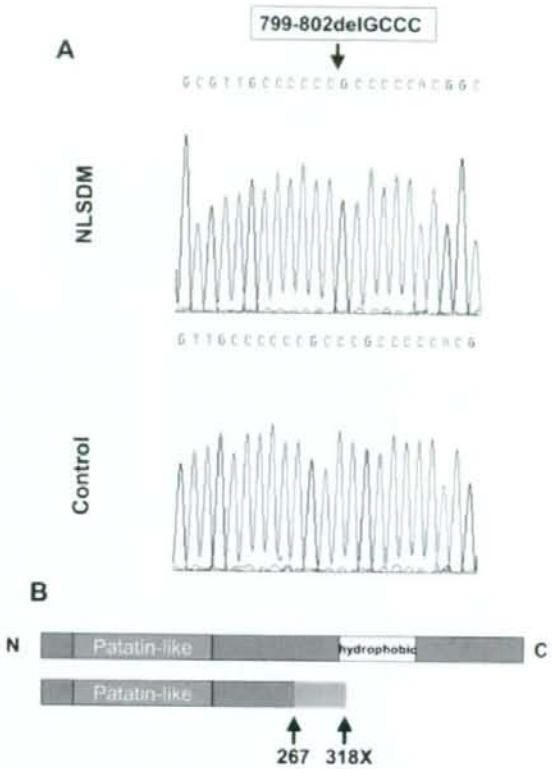

FIG. 2. ATGL mutation in the patient with NLSDM. The direct sequence of ATGL cDNA reveals that the patient is a homozygote for a 4-bp deletion (799–802delGCCC) (A), leading to frameshift (*green*) and a premature stop codon at amino acid position 318, which results in the lack of the C terminus of the protein including the hydrophobic domain (B).

occurred at a unique GC sequence (GCCCCCCCGCCCGCCCC) of the gene, near which individuals 1 and 2 reported by Fischer *et al.* (15) also had heterozygous and homozygous single base pair deletions, respectively. We detected no mutation in the sequence of the CGI-58 gene, another causative gene of NLSDs (4) (data not shown).

Localization of endogenous ATGL in peripheral blood leukocytes and GFP-fused ATGL expression in NLSDM fibroblasts

Peripheral blood leukocytes from the patient showed cytoplasmic vacuoles (Jordans' anomaly) (Fig. 3A) and Oil red O-positive LDs (Fig. 3B). Immunostaining suggested that endogenous ATGL of the patient was located in the cytoplasm homogeneously and not around the rims of LDs (Fig. 3D), whereas endogenous ATGL protein was not clearly detected in control leukocytes (Fig. 3E). We next investigated the distribution of GFP-fused control and NLSDM ATGL proteins in the patient's fibroblasts. It has been reported that endogenous ATGL is localized around the rims of LDs (13). By contrast, localization of overexpressed ATGL is unclear, such as homogenous distribution (10) or a granular appearance (20) in the cytoplasm. In the present study, GFP-control ATGL protein was located in cytoplasm and appeared as a ring shape around LDs. By contrast, GFP-fused NLSDM ATGL was homogeneously located in the nucleus and cytoplasm, and LDs remained after transfection, suggesting that NLSDM ATGL is not capable of approaching and degrading LDs (Fig. 3F).

Effects of control and NLSDM ATGL expression on the lipid contents in fibroblasts and different distribution of both ATGL

To investigate the effects of the mutation on lipid degradation activity, we carried out transfection studies using COS7 cells (Fig. 4, A, C, and D) or fibroblasts from the patient's skin (Fig. 4B). Transfection of control ATGL in NLSDM fibroblasts significantly reduced cellular lipid accumulation. Lipid contents in NLSDM ATGL-transfected cells showed no significant difference from those in β-galactosidase (LacZ)-transfected cells (Fig. 4B). We next investigated intracellular distribution of both control and NLSDM ATGL. In total cell extracts, NLSDM ATGL-transfected COS7 cells showed similar lipase activity to control. In addition, both ATGL activities were stimulated by CGI-58

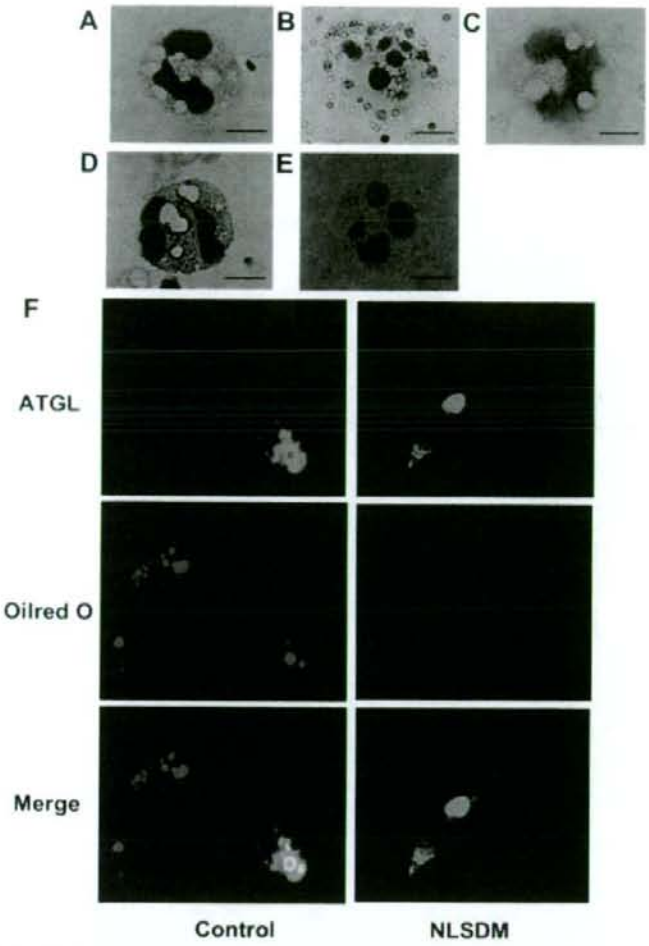

FIG. 3. Localization of endogenous ATGL in peripheral blood leukocytes obtained from an NLSDM patient. Leukocytes from the patient's peripheral blood show cytoplasmic lipid droplets (Jordans' anomaly). A, Hematoxylin and eosin; *bar*, 5 μm. B, Oil red O; *bar*, 5 μm. Immunoreactivity was visualized with 3, 3′-diaminobenzidine tetrahydrochloride staining (*brown*) and counterstained with hematoxylin (*violet-blue*). C, A negative control; *bar*, 5 μm. D, NLSDM leukocytes; *bar*, 5 μm. E, Control leukocytes; *bar*, 5 μm. F, Overexpression of control and NLSDM ATGL is differently distributed in NLSDM fibroblasts. Fibroblasts established from the NLSDM patient were transfected with plasmids expressing GFP-control ATGL or GFP-NLSDM ATGL and assessed by confocal laser-scanning microscopy.

(Fig. 4C). In contrast, LD-associated NLSDM ATGL activity was significantly lower than control (Fig. 4D).

Effects of expression of deletion mutants of ATGL on LDs in NLSDM fibroblasts

To investigate details of the role of the C-terminal region in lipid degradation, we made a series of C-terminal deletion mutants (Fig. 5A) and carried out transfection studies. In total cell extracts prepared from transfected COS7 cells, deletion mutants (mutant 1–3) showed similar lipase activities, which were stimulated by CGI-58. On the contrary, mutant 4, which lacks total hydrophobic region and partial patatin-like phospholipase domain, showed almost no lipase activity or no enhancing effect of CGI-58 (Fig. 5B). LDs in transfected cells was diminished completely by control ATGL and mostly diminished by mutants 1 and 2, which have the intact hydrophobic domain. In contrast, the expression of mutants 3 and 4 showed no effect on LDs and significantly higher intracellular lipid contents (Fig. 6).

Discussion

CDS (MIM 27630) (2, 3) is an autosomal recessive form of NLSD characterized by the presence of ichthyosis and intracellular triglyceride droplets in most tissues. In 2001 Lefevre *et al.* (4) identified CGI-58, of the esterase/thioesterase/lipase superfamily, as a causative gene using linkage-disequilibrium analysis. CGI-58 binds to intracellular LDs together with perilipin A (21, 22) and is demonstrated to stimulate ATGL activity (12). ATGL, also known as desnutrin or calcium-independent phospholipase A2ζ, has been reported by three independent groups (9–11) and shown to have a pivotal role in the initial step of triglyceride hydrolysis. The N-terminal part of ATGL contains a patatin-like phospholipase domain and GXSXG consensus sequence for serine lipases. On the other hand, Brummer lipase, a Drosophila homolog of human ATGL, has a pivotal region for localizing around LDs called the Brummer box (23). Smirnova *et al.* (13) showed that an ATGL mutant-S47A in phospholipase domain, which lacks lipase activity, failed to decrease the LD size but still was present around the LDs. These results suggest that ATGL also contains the putative lipid-binding site. Recently Fischer *et al.* (15) demonstrated mutations of ATGL in a NLSD subgroup with myopathy and without ichthyosis (NLSDM). These mutations lead to a truncated ATGL protein with a patatin-like phospholipase domain but without the C-terminal region including the hydrophobic amino acid-rich domain (residues 309–391). They showed that whole-cell neutral lipase activity in NLSDM fibroblasts was the same as in control fibroblasts but that lipid droplet-associated lipase activity was eventually diminished. However, the mutated ATGL of individual 2 they used in the lipase studies lacks the C-terminal half of the protein; therefore, it is possible that the defective part other than hydrophobic region plays a role in ATGL association with LDs. In addition, it is also possible that a C-terminal nonsense sequence caused by a frameshift of this mutant ATGL inhibits the targeting of ATGL to LDs. The ATGL of our patient showed a novel mutation and lacked the C-terminal hydrophobic domain but also had a nonsense sequence at C terminus (Fig.

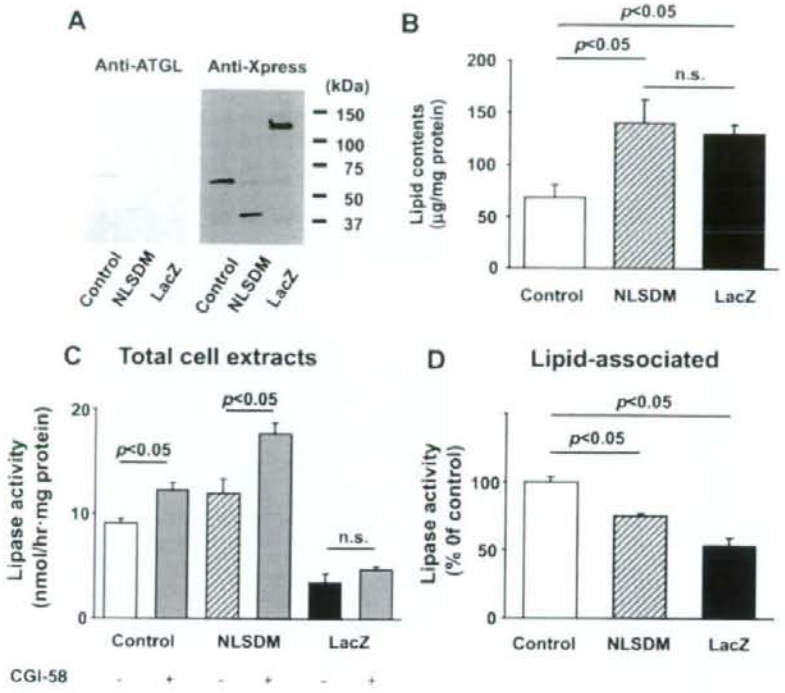

FIG. 4. Effect of overexpression of control or NLSDM ATGL on lipid contents and lipase activities in NLSDM fibroblasts. A, Western blotting analysis of ATGL expression in transfected NLSDM fibroblasts. Fibroblasts established from the NLSDM patient were transfected with cytomegalovirus promoter-driven expression plasmids containing control, NLSDM ATGL, and β-galactosidase (LacZ). B, Intracellular lipid contents in transfected NLSDM fibroblasts. Lipase activities in total cell extracts (C) and lipid-associated fractions (D) were determined with COS7 cells as described in *Patients and Methods*. Values are means ± SE ($n = 4–6$).

2B). In the present study, we sought to confirm that the C-terminal region of ATGL that includes the hydrophobic domain was essential for localization around LDs.

First, we checked the localization of ATGL in the patient's leukocytes with Jordans' anomaly. Smirnova *et al.* (13) reported that endogenous ATGL showed a pattern of small rings that colocalized with tail-interacting protein of 47 kDa. Contrarily, the patient's ATGL was located homogenously in cytoplasm of peripheral blood leukocytes (Fig. 3D). We used a GFP fusion expression plasmid and the patient's fibroblasts to determine the distribution of control and the patient's mutant ATGL. GFP-control ATGL fusion protein was located ring-like around small LDs, whereas GFP-NLSDM ATGL showed homogenous distribution in the cytoplasm and residual LDs. (Fig. 3F). Next, we investigated the effects of the mutation on intracellular localization and lipid degradation activity. NLSDM fibroblasts transfected with NLSDM ATGL showed significantly higher lipid contents than control ATGL-transfected cells. In COS7 cells transfected with NLSDM ATGL, LD-associated lipase activities were significantly lower than control-transfected cells, whereas lipase activities in total cell extracts show no difference including enhancing effect of CGI-58. These results suggest that the patient's ATGL was not capable of association with LDs, thereby resulting in inefficient lipid degradation. Then we generated a series of ATGL deletion mutants (Fig. 5A) to undertake a detailed analysis of the C-terminal part of ATGL protein without an additional nonsense sequence. Mutants 1 and 2, which have the intact hydrophobic domain, showed similar lipase activity in total cell extracts to control ATGL and trace amount of LDs. In contrast, mutant 3, which lacks partial hydrophobic domain, showed significantly higher lipase activity than control but was not capable of degrading LDs to the same extent as NLSDM ATGL, and mutant 4, which lacks complete hydrophobic domain and partial lipase domain (Figs. 5B and 6). These results suggested that the C-terminal part of ATGL, in particular the hydrophobic region, was essential for association with LDs. Granneman *et al.* (24) proposed a working model of lipolytic trafficking. ATGL is both cytoplasmic and bound to LDs in the basal state. Protein kinase A activation by stimulation causes phosphorylation of perilipin A, which frees CGI-58 to recruit and activate ATGL on the surface of LDs, thereby leading to triglyceride breakdown. According to our present study, the C-terminal hydrophobic domain of ATGL does not seem to be important for interaction with CGI-58. We then carried out an immunoprecipitation study but were not able to detect any association of control or mutant ATGL with CGI-58, maybe because of the limited detection sensitivity (data not shown). The effects of the N-terminal part of ATGL including patatin-like phospholipase domain and residues 178–267 (between the patatin-like domain and a C-terminal nonsense sequence caused by a frame shift) on its interaction with CGI-58 remain to be elucidated in detail.

The two patients reported here showed similar clinical features to those of individual 2 reported by Fischer *et al.* (15), such as cardiomyopathy and chronic pancreatitis besides myopathy and liver dysfunction. In addition, both had hypothyroidism. All these characteristics were probably associated with lipid deposition because LDs were seen in cardiac muscle (supplemental Fig. 1B), an atrioventricular node (supplemental Fig. 1C), and the thyroid gland (supplemental Fig. 1F). Notably, the two cases here and individual 2 had type 2 diabetes mellitus. Several investigators reported that intramyocellular lipid content is correlated with insulin resistance in humans (25, 26). However, our female patient showed no insulin resistance from the euglycemic-hyperinsulinemic clamp study and homeostasis model assessment for insulin resistance. Instead, she showed decreasing insulin secretory capacity with age (supplemental Fig. 1A). It is possible that lipid deposition in pancreatic cells (supplemental Fig. 1, D and E) caused dysfunction, thereby leading to the onset

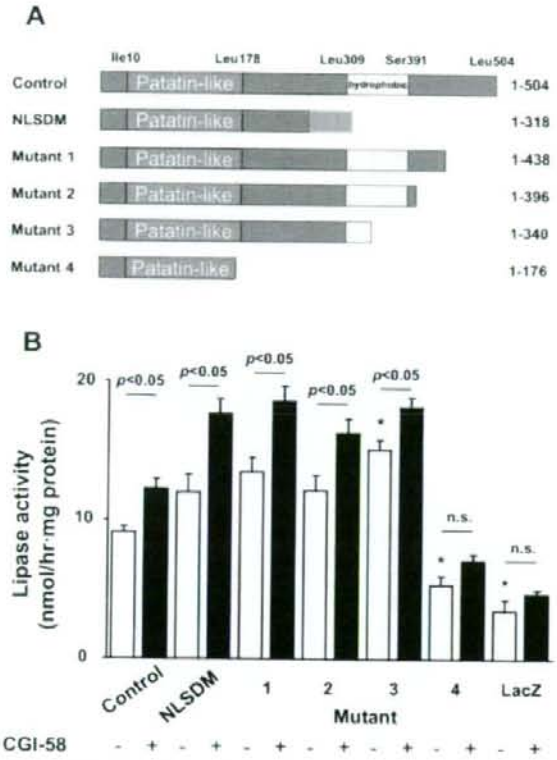

FIG. 5. Effects of C-terminal deletion mutants on lipase activities in transfected COS7 cells. A, Predicted structures of control, NLSDM, and C-terminal truncated ATGL mutants. The *red*, *yellow*, and *green* boxes indicate a patatin-like phospholipase domain, a hydrophobic region, and frameshift, respectively. *Numbers* indicate amino acid residues of ATGL. B, Lipase activities in total cell extracts from COS7 cells transfected with various ATGL mutants with or without CGI-58. *, $P < 0.05$ *vs.* control. n.s., Not significant.

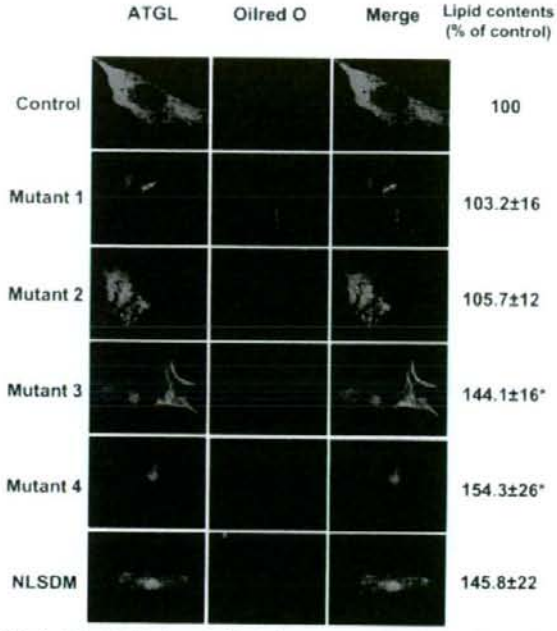

FIG. 6. Hydrophobic domain-deleted mutants cause residual LDs. Control, NLSDM, and truncated ATGLs were subcloned into GFP expression plasmids. NLSDM fibroblasts were transiently transfected with recombinant plasmids and stained with Oil red O and assessed by confocal laser-scanning microscopy. Intracellular lipid contents were determined as described in *Patients and Methods*. *, $P < 0.05$ *vs.* control.

of diabetes mellitus. On the other hand, this notion is inconsistent with the finding that ATGL knockout mice showed increased glucose tolerance and increased insulin sensitivity, regardless of lipid deposition in muscle (14). The clinical significance of ATGL on glucose metabolism should be investigated and hopefully revealed in future studies.

In summary, we have identified a novel homozygous mutation of the ATGL gene in a NLSDM patient. The mutation caused a lack of the C-terminal of the protein including the hydrophobic region. A lack of the C-terminal region of ATGL leads to dissociation from LDs and lipid deposition, whereas gene supplementation diminished LDs in NLSDM fibroblasts.

Acknowledgments

We thank Mikiko Sato for her research assistance. We also thank Ms. Eri Nagashima and Ms. Tamaki Amano for secretarial help.

Address all correspondence and requests for reprints to: Kumihisa Kobayashi, M.D., Ph.D., Department of Medicine and Bioregulatory Science, Graduate School of Medical Sciences, Kyushu University, 3-1-1 Maidashi, Higashi-ku, Fukuoka 812-8582 Japan. E-mail: nihisak@med.kyushu-u.ac.jp.

Disclosure Information: All authors have nothing to declare.

References

1. **Jordans GH** 1953 The familial occurrence of fat containing vacuoles in the leukocytes diagnosed in two brothers suffering from dystrophia musculorum progressiva (ERB.). Acta Med Scand 145:419–423
2. **Dorfman ML, Hershko C, Eisenberg S, Sagher F** 1974 Ichthyosiform dermatosis with systemic lipidosis. Arch Dermatol 110:261–266
3. **Chanarin I, Patel A, Slavin G, Wills EJ, Andrews TM, Stewart G** 1975 Neutral-lipid storage disease: a new disorder of lipid metabolism. Br Med J 1:553–555
4. **Lefevre C, Jobard F, Caux F, Bouadjar B, Karaduman A, Heilig R, Lakhdar H, Wollenberg A, Verret JL, Weissenbach J, Ozguc M, Lathrop M, Prud'homme JF, Fischer J** 2001 Mutations in CGI-58, the gene encoding a new protein of the esterase/lipase/thioesterase subfamily, in Chanarin-Dorfman syndrome. Am J Hum Genet 69:1002–1012
5. **Lai CH, Chou CY, Ch'ang LY, Liu CS, Lin W** 2000 Identification of novel human genes evolutionarily conserved in *Caenorhabditis elegans* by comparative proteomics. Genome Res 10:703–713
6. **Wessalowski R, Schroten H, Neuen-Jacob E, Reichmann H, Melnik BC, Lenard HG, Voit T** 1994 Multisystem triglyceride storage disorder without ichthyosis in two siblings. Acta Paediatr 83:93–98
7. **Haemmerle G, Zimmermann R, Hayn M, Theussl C, Waeg G, Wagner E, Sattler W, Magin TM, Wagner EF, Zechner R** 2002 Hormone-sensitive lipase deficiency in mice causes diglyceride accumulation in adipose tissue, muscle, and testis. J Biol Chem 277:4806–4815
8. **Osuga J, Ishibashi S, Oka T, Yagyu H, Tozawa R, Fujimoto A, Shionoiri F, Yahagi N, Kraemer FB, Tsutsumi O, Yamada N** 2000 Targeted disruption of hormone-sensitive lipase results in male sterility and adipocyte hypertrophy, but not in obesity. Proc Natl Acad Sci USA 97:787–792
9. **Zimmermann R, Strauss JG, Haemmerle G, Schoiswohl G, Birner-Gruenberger R, Riederer M, Lass A, Neuberger G, Eisenhaber F, Hermetter A, Zech-**

ner R 2004 Fat mobilization in adipose tissue is promoted by adipose triglyceride lipase. Science 306:1383–1386
10. Villena JA, Roy S, Sarkadi-Nagy E, Kim KH, Sul HS 2004 Desnutrin, an adipocyte gene encoding a novel patatin domain-containing protein, is induced by fasting and glucocorticoids: ectopic expression of desnutrin increases triglyceride hydrolysis. J Biol Chem 279:47066–47075
11. Jenkins CM, Mancuso DJ, Yan W, Sims HF, Gibson B, Gross RW 2004 Identification, cloning, expression, and purification of three novel human calcium-independent phospholipase A2 family members possessing triacylglycerol lipase and acylglycerol transacylase activities. J Biol Chem 279:48968–48975
12. Lass A, Zimmermann R, Haemmerle G, Riederer M, Schoiswohl G, Schweiger M, Kienesberger P, Strauss JG, Gorkiewicz G, Zechner R 2006 Adipose triglyceride lipase-mediated lipolysis of cellular fat stores is activated by CGI-58 and defective in Chanarin-Dorfman syndrome. Cell 3:309–319
13. Smirnova E, Goldberg EB, Makarova KS, Lin L, Brown WJ, Jackson CL 2006 ATGL has a key role in lipid droplet/adiposome degradation in mammalian cells. EMBO Rep 7:106–113
14. Haemmerle G, Lass A, Zimmermann R, Gorkiewicz G, Meyer C, Rozman J, Heldmaier G, Maier R, Theussl C, Eder S, Kratky D, Wagner EF, Klingenspor M, Hoefler G, Zechner R 2006 Defective lipolysis and altered energy metabolism in mice lacking adipose triglyceride lipase. Science 312:734–737
15. Fischer J, Lefevre C, Morava E, Mussini JM, Laforet P, Negre-Salvayre A, Lathrop M, Salvayre R 2007 The gene encoding adipose triglyceride lipase (PNPLA2) is mutated in neutral lipid storage disease with myopathy. Nat Genet 39:28–30
16. Imamura M, Inoguchi T, Ikuyama S, Taniguchi S, Kobayashi K, Nakashima N, Nawata H 2002 ADRP stimulates lipid accumulation and lipid droplet formation in murine fibroblasts. Am J Physiol Endocrinol Metab 283:E775–E783
17. Lehner R, Verger R 1997 Purification and characterization of a porcine liver microsomal triacylglycerol hydrolase. Biochemistry 36:1861–1868
18. Riccobon A, Gunelli R, Ridolfi R, De Paola F, Flamini E, Fiori M, Saltutti C, Petrini M, Frammenghi L, Stefanelli M, Granato AM, Cuzzocrea DE, Amadori D 2004 Immunosuppression in renal cancer: differential expression of signal transduction molecules in tumor-infiltrating, near-tumor tissue, and peripheral blood lymphocytes. Cancer Invest 22:871–877
19. Yokoyama H, Emoto M, Mori K, Araki T, Teramura M, Koyama H, Shoji T, Inaba M, Nishizawa Y 2006 Plasma adiponectin level is associated with insulin-stimulated nonoxidative glucose disposal. J Clin Endocrinol Metab 91:290–294
20. Baulande S, Lasnier F, Lucas M, Pairault J 2001 Adiponutrin, a transmembrane protein corresponding to a novel dietary-and obesity-linked mRNA specifically expressed in the adipose lineage. J Biol Chem 276:33336–33344
21. Yamaguchi T, Omatsu N, Matsushita S, Osumi T 2004 CGI-58 interacts with perilipin and is localized to lipid droplets. Possible involvement of CGI-58 mislocalization in Chanarin-Dorfman syndrome. J Biol Chem 279:30490–30497
22. Subramanian V, Rothenberg A, Gomez C, Cohen AW, Garcia A, Bhattacharyya S, Shapiro L, Dolios G, Wang R, Lisanti MP, Brasaemle DL 2004 Perilipin A mediates the reversible binding of CGI-58 to lipid droplets in 3T3-L1 adipocytes. J Biol Chem 279:42062–42071
23. Gronke S, Mildner A, Fellert S, Tennagels N, Petry S, Muller G, Jackle H, Kuhnlein RP 2005 Brummer lipase is an evolutionary conserved fat storage regulator in Drosophila. Cell Metab 1:323–330
24. Granneman JG, Moore HP, Granneman RL, Greenberg AS, Obin MS, Zhu Z 2007 Analysis of lipolytic protein trafficking and interactions in adipocytes. J Biol Chem 282:5726–5735
25. Perseghin G, Scifo P, De Cobelli F, Pagliato E, Battezzati A, Arcelloni C, Vanzulli A, Testolin G, Pozza G, Del Maschio A, Luzi L 1999 Intramyocellular triglyceride content is a determinant of *in vivo* insulin resistance in humans: a 1H-13C nuclear magnetic resonance spectroscopy assessment in offspring of type 2 diabetic parents. Diabetes 48:1600–1606
26. Jacob S, Machann J, Rett K, Brechtel K, Volk A, Renn W, Maerker E, Matthaei S, Schick F, Claussen CD, Haring HU 1999 Association of increased intramyocellular lipid content with insulin resistance in lean nondiabetic offspring of type 2 diabetic subjects. Diabetes 48:1113–1119

Available online at www.sciencedirect.com
ScienceDirect
Metabolism Clinical and Experimental 57 (2008) 1038–1045
Metabolism
Clinical and Experimental
www.metabolismjournal.com

Differential effect of sulfonylureas on production of reactive oxygen species and apoptosis in cultured pancreatic β-cell line, MIN6

Fumi Sawada, Toyoshi Inoguchi*, Hirotaka Tsubouchi, Shuji Sasaki, Masakazu Fujii, Yasutaka Maeda, Hidetaka Morinaga, Masatoshi Nomura, Kunihisa Kobayashi, Ryoichi Takayanagi

Department of Medicine and Bioregulatory Science, Graduate School of Medical Sciences, Kyushu University, Fukuoka 812-8582, Japan

Received 24 August 2007; accepted 10 January 2008

Abstract

Sulfonylureas are considered to cause β-cell apoptosis. However, it is unclear how this occurs and whether there is a difference in such effects among various sulfonylureas. Here, we examined the effects of various sulfonylureas and a short-acting insulin secretagogue, nateglinide, on oxidative stress and apoptosis using the β-cell line MIN6. After cultured MIN6 cells were exposed to various concentrations of sulfonylureas (glibenclamide, glimepiride, and gliclazide) or nateglinide, intracellular production of reactive oxygen species (ROS) was evaluated by staining with 2′,7′-dichlorofluorescein diacetate. The effect of these agents on apoptosis was also evaluated by the terminal deoxynucleotidyl transferase–mediated deoxyuridine triphosphate–biotin nick-end labeling technique. Exposure of β-cells to glibenclamide, glimepiride, and nateglinide significantly increased intracellular ROS production in a concentration-dependent manner (0.1-10 μmol/L). These effects were completely blocked by nicotinamide adenine dinucleotide phosphate [NAD(P)H] oxidase inhibitors (diphenylene iodonium or apocynin) or a protein kinase C inhibitor (calphostin C). After exposure to these agents for 48 hours, the numbers of apoptotic cells were also significantly increased. These effects were significantly blocked by apocynin and antioxidant *N*-acetyl-L-cysteine. In contrast, exposure to any concentrations of gliclazide did not affect either intracellular ROS production or the numbers of apoptotic cells. Sulfonylureas (glibenclamide and glimepiride, but not gliclazide) and nateglinide stimulated ROS production via protein kinase C–dependent activation of NAD(P)H oxidase and consequently caused β-cell apoptosis in vitro. Because of the lack of such adverse effects, gliclazide may have a benefit in the preservation of functional β-cell mass.

1. Introduction

The natural history of type 2 diabetes mellitus is characterized by progression of the disease. The contribution of relative insulin deficiency to the establishment of overt diabetes or the progression of the disease is now widely accepted and is probably due to a decrease in the functional β-cell mass [1,2]. In a pathophysiological condition, persistent elevation of the glucose concentration impairs β-cell function and induces β-cell apoptosis, so-called glucose toxicity [3,4]. One potential mechanism for glucose toxicity is that of excessive formation of reactive oxygen species (ROS) in β-cells. Persistent excessive ROS formation has been reported to cause decreased insulin gene expression via a loss of the transcription factors pancreatic and duodenal homeobox protein 1 (PDX-1) and musculoaponeurotic fibrosarcoma oncogene homologue A (MafA) [5], and has also been reported to accelerate rates of β-cell apoptosis [6,7]. Accumulating evidence suggests that oxidative stress is increased in pancreatic β-cells in diabetic animal models and diabetic patients [8-11].

Sulfonylureas are commonly used in the treatment of type 2 diabetes mellitus because these drugs effectively reduce blood glucose levels in type 2 diabetes mellitus. Despite their beneficial effects, continuous use of sulfonylureas may cause β-cell dysfunction and apoptosis. Several reports have suggested that sustained enhancement of Ca^{2+} influx by sulfonylureas may be a causative mechanism for β-cell apoptotic cell death [12,13]. On the other hand, we recently

* Corresponding author. Tel.: +81 92 642 5284; fax: +81 92 642 5287.
E-mail address: toyoshi@intmed3.med.kyushu-u.ac.jp (T. Inoguchi).

0026-0495/$ - see front matter © 2008 Elsevier Inc. All rights reserved.
doi:10.1016/j.metabol.2008.01.038

reported that the sulfonylurea glibenclamide, as well as high glucose levels, stimulated production of ROS in the pancreatic β-cell line MIN6 [14]. Thus, this mechanism might, in part, account for β-cell dysfunction and apoptosis induced by sulfonylureas. It is therefore important to evaluate whether sulfonylureas induce β-cell apoptosis via increases in ROS production and to evaluate whether there is a difference in such adverse effects among various sulfonylureas and other insulin secretagogues. In this context, this study was undertaken to examine the dose-dependent effects of the classic sulfonylurea glibenclamide, the new-generation sulfonylureas gliclazide and glimepiride, and a short-acting insulin secretagogue, nateglinide, on ROS production and apoptosis using the pancreatic β-cell line MIN6 and mouse islets.

2. Materials and methods

2.1. Materials and chemicals

2′,7′-Dichlorofluorescein diacetate (DCF-DA) was purchased from Molecular Probes (Eugene, OR). Calphostin C, diphenyleneiodonium chloride, *N*-acetyl-L-cysteine (NAC), rotenone, oxypurinol, and *N*-methyl-L-arginine were purchased from Sigma (St Louis, MO). Apocynin was purchased from Extrasynthese (Lyon, France). A guinea pig anti-insulin antibody was purchased from Dako (Carpinteria, CA), and an anti–guinea pig immunoglobulin G was purchased from Sigma. Glibenclamide and glimepiride were kindly provided by Sanofi-Aventis (Paris, France). Gliclazide was kindly provided by Dainippon Sumitomo Pharma (Osaka, Japan). Nateglinide was kindly provided by AJINOMOTO (Tokyo, Japan).

2.2. Cell culture

Pancreatic β-cell line MIN6 cells were kindly provided by Dr S Seino (Division of Cellular and Molecular Medicine, Kobe University Graduate School of Medicine, Kobe, Japan) and Dr E Araki (Department of Metabolic Medicine, Faculty of Medical and Pharmaceutical Sciences, Kumamoto University, Kumamoto, Japan). The MIN6 cells were maintained in DMEM containing 15% fetal bovine serum (FBS), 100 U/mL penicillin, 100 μg/mL streptomycin, and 25 mmol/L glucose at 37°C in an atmosphere of 95% O_2/5% CO_2.

2.3. Mouse islets isolation and culture

Pancreatic islets were isolated from 20-week–old B6 mice by collagenase digestion followed by gradient density centrifugation. Briefly, mice were killed by cervical dislocation. The pancreas was exposed and injected with Hanks balanced salt solution containing 2 mg/mL collagenase (Collagenase CLS-4; Worthington Biochemical, Lakewood, NJ) via common bile duct until distended. Digestion was performed at 37°C. Pancreas was mechanically disrupted by passing through a metal needle, and islets were purified on Histopaque (Sigma) gradients by centrifugation. Islets were handpicked and transferred into CMRL-1066 containing 10% FBS, 100 U/mL penicillin, 100 μg/mL streptomycin, 2 mmol/L L-glutamine, and 5.5 mmol/L glucose at 37°C in an atmosphere of 95% O_2/5% CO_2.

Care and maintenance of all animals were in accordance with the principles of laboratory animal care and guidelines of institutional Animal Policy and Welfare Committee.

2.4. Evaluation of ROS production in MIN6 cells

2′,7′-Dichlorofluorescein diacetate was used to evaluate intracellular oxidant formation as previously reported [14]. For experiments, the cells were placed into glass-bottom culture dishes (MatTek, Ashland, MA) and cultured in DMEM containing 15% FBS and 25 mmol/L glucose. When the cells reached the loose confluent layer, the medium was replaced with DMEM containing 1% FBS and 5.5 mmol/L glucose with glibenclamide, gliclazide, glimepiride, or nateglinide for 2, 6, 12, 18, and 24 hours. All pharmacological compounds were prepared in dimethyl sulfoxide or water. The final concentration of dimethyl sulfoxide in the solution was always 0.1%. The cells were then loaded with 2 μmol/L DCF-DA, a nonfluorescent compound that freely permeates cells and interacts with intracellular oxidants to form fluorescence compound DCF. After 20 minutes, digital images of DCF fluorescence were obtained with a fluorescence microscope system (Olympus, Tokyo, Japan) at an excitation wavelength of 488 nm (argon laser) using a 515-nm long-pass emission filter. The obtained fluorescence images were converted to gray-scale images using Photoshop software (Adobe Systems, San Jose, CA), and the fluorescence intensities were quantitatively analyzed using National Institutes of Health image software (Fortner Research, Sterling, VA).

2.5. Detection and quantification of apoptosis of MIN6

Apoptosis of cells was evaluated by terminal deoxynucleotidyl transferase–mediated deoxyuridine triphosphate nick-end labeling (TUNEL) assay, as previously described. For experiments, MIN6 cells were placed into glass-bottom culture dishes (MatTek) and cultured in DMEM containing 15% FBS and 25 mmol/L glucose. When the cells reached the loose confluent layer, the medium was replaced with DMEM containing 1% FBS and 5.5 mmol/L glucose with glibenclamide with or without apocynin (100 μmol/L) or NAC (1 mmol/L), gliclazide, glimepiride, or nateglinide. After incubation for 48 hours, the cells were fixed in 4% paraformaldehyde in phosphate-buffered saline. The glasses were then processed for the TUNEL assay. An In Situ Apoptosis Detection Kit from TaKaRa Bio (Otsu, Japan) was used according to the manufacturer's instructions. The cells were treated with H_2O_2 and incubated with the reaction mixture containing terminal deoxynucleotidyl transferase and digoxigenin-conjugated deoxyuridine triphosphate for 1 hour at 37°C. Labeled DNA was visualized with peroxidase-conjugated anti-digoxigenin antibody using 3,3′-diaminobenzidine as the chromogen. After washing in distilled water, the cells were counterstained in 0.5% methyl green.

2.6. Detection and quantification of apoptosis of islets

Apoptosis of cells was also evaluated by TUNEL assay, as above. For experiments, cultured mouse islets were transferred to CMRL-1066 containing 1% FBS and 5.5 mmol/L glucose with glibenclamide with or without apocynin or NAC, gliclazide, glimepiride, or nateglinide. After incubation for 48 hours, the islets were dissociated with trypsin-EDTA (Sigma). After washing, cells were prepared by cytospin (Shandon, Pittsburgh, PA) on glass slide and fixed in 4% paraformaldehyde in phosphate-buffered saline. An In situ Apoptosis Detection Kit (TaKaRa) was used as above. After 3,3'-diaminobenzidine staining and washing, immunostaining for insulin was performed to distinguish β-cell. Islets were stained with a guinea pig anti-insulin antibody (Dako), followed by alkaline phosphatase conjugated anti-guinea pig immunoglobulin G (Sigma) using alkaline phosphatase substrate kit III (Vector Laboratories, Burlingame, CA) as the chromogen.

2.7. Statistical analysis

All data are expressed as means ± SEM. Statistical analysis was performed by analysis of variance followed by post hoc comparison tests.

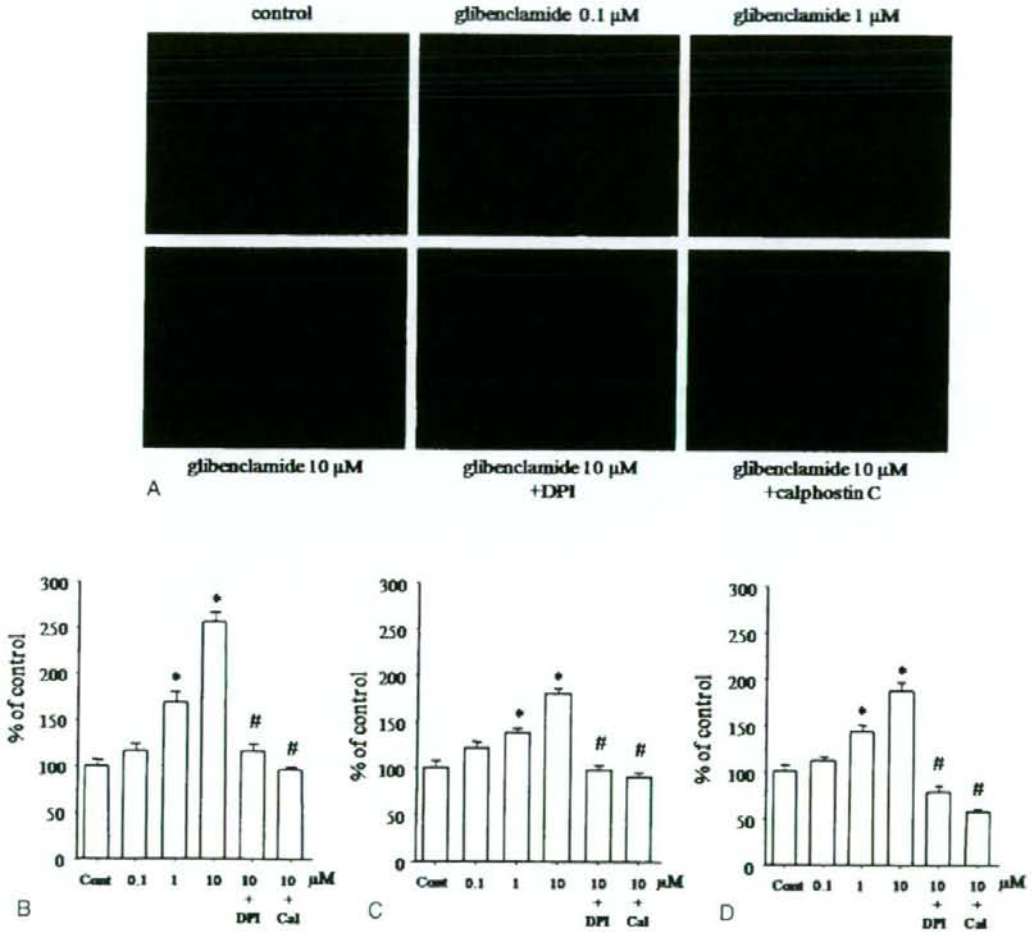

Fig. 1. Effect of glibenclamide, glimepiride, and nateglinide on production of ROS in cultured pancreatic β-cell line MIN6. The MIN6 cells were cultured in test media containing 1% FBS and 5.5 mmol/L glucose with or without various concentrations of glibenclamide, glimepiride, and nateglinide for 24 hours. Diphenyleneiodonium chloride or calphostin C was incubated simultaneously with these agents (10 μmol/L) for the last 2 hours. After 24 hours of incubation, DCF-DA was added at a concentration of 2 μmol/L. After 20 minutes, digital images of DCF fluorescence were obtained with a fluorescence microscope system. A, Representative fluorescent images of glibenclamide-treated cells. Quantitative analysis of the fluorescence intensities on the images of glibenclamide-treated (B) (n = 12), glimepiride-treated (C) (n = 12), and nateglinide-treated cells (D) (n = 10). *$P < .01$ vs nontreated cells. #$P < .01$ vs sulfonylureas- or nateglinide (10 μmol/L)-treated cells each. Data are expressed as mean percentage of control ± SEM. Cal indicates calphostin C; Cont, control.

3. Results

3.1. Effects of sulfonylureas and nateglinide on intracellular ROS production in MIN6 cells

Exposure of the MIN6 cells to glibenclamide, glimepiride, and nateglinide for 24 hours induced a significant increase in intracellular ROS production in a concentration-dependent manner (0.1-10 μmol/L) (Fig. 1A-D, respectively). These stimulatory effects were completely blocked by the incubation with a nicotinamide adenine dinucleotide phosphate [NAD(P)H] oxidase inhibitor, diphenyleneiodonium chloride (1 μmol/L), or a protein kinase C (PKC) inhibitor, calphostin C (500 nmol/L). Other flavoprotein inhibitors including rotenone (100 μmol/L), oxypurinol (100 μmol/L), or *N*-methyl-L-arginine (10 μmol/L) did not significantly affect ROS production induced by these agents (data not shown). In contrast, exposure of the cells to gliclazide did not induce a significant increase in ROS production at any concentration (0.1-10 μmol/L) (Fig. 2A, B). As shown in Fig. 3, when the intensity of the stimulatory effect was compared among these agents at the concentration of 10 μmol/L, the stimulatory effect of glibenclamide was significantly greater than that of glimepiride and nateglinide. These stimulatory effects were observed at 2 hours after the start of incubation and lasted for up to 24 hours, but no stimulatory effect of gliclazide was found at any incubation time (Fig. 4).

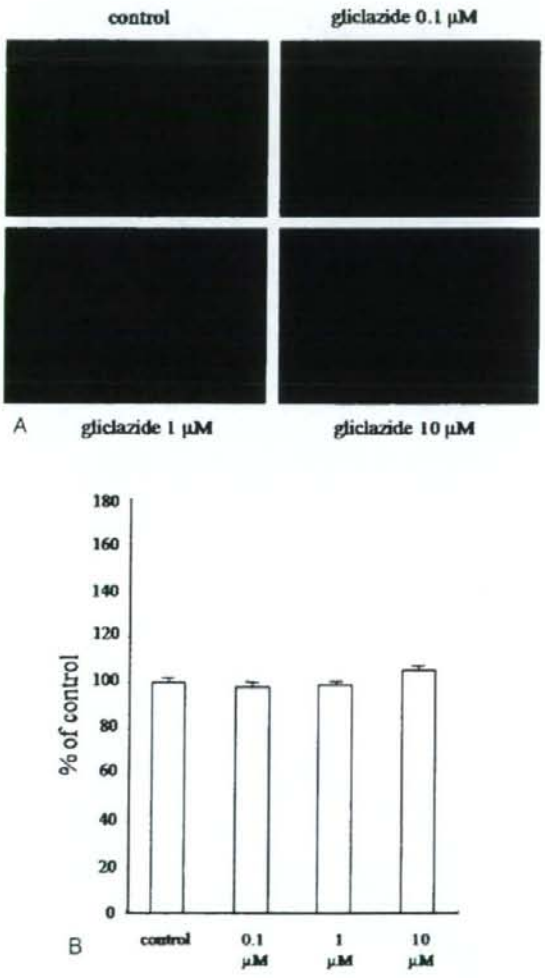

Fig. 2. Effect of gliclazide on ROS production in cultured pancreatic β-cell line MIN6. A, Representative fluorescence images of gliclazide-treated cells. B, Quantitative analysis of the fluorescence intensities on the images of gliclazide-treated cells. Data are expressed as mean percentage of control ± SEM (n = 10).

3.2. Effects of sulfonylureas and nateglinide on β-cell apoptosis

As shown in Fig. 5A, B, exposure of the cells to glibenclamide, glimepiride, and nateglinide at the concentration of 10 μmol/L for 48 hours induced a significant increase in the number of brown-colored TUNEL-positive cells compared with control. In parallel with the results of ROS production, the stimulatory effects of glibenclamide on apoptosis were significantly greater than those of glimepiride and nateglinide. In contrast, exposure of the cells to gliclazide did not induce a significant increase in the number of apoptotic cells (Fig. 5A, B). Simultaneous addition of both the NAD(P)H oxidase apocynin (100 μmol/L) and the antioxidant NAC (1 mmol/L) significantly inhibited glibenclamide-induced apoptosis (Fig. 6).

3.3. Effects of sulfonylureas and nateglinide on islet cell apoptosis

As shown in Fig. 7A, exposure of the islet cells to glibenclamide, glimepiride, and nateglinide at the concentration of 10 μmol/L for 48 hours also induced a significant increase in the number of TUNEL-positive cells compared with controls. Again, exposure of the islet cells to gliclazide did not induce a significant increase in the number of apoptotic cells. Simultaneous addition of both the apocynin and NAC significantly inhibited glibenclamide-induced islet cell apoptosis (Fig. 7B).

4. Discussion

Although sulfonylureas are widely used for the treatment of type 2 diabetes mellitus, it is of concern that continuous use of sulfonylureas may cause β-cell dysfunction and apoptosis. In a prospective study comparing insulin and glibenclamide treatment of type 2 diabetes mellitus, it was shown that treatment with insulin preserved β-cell function more effectively than glibenclamide [15]. Thus, given the possible deleterious effects of sulfonylureas, it is important to understand how sulfonylureas may cause β-cell dysfunction and apoptosis, and whether there is a difference in such effects among various sulfonylureas.

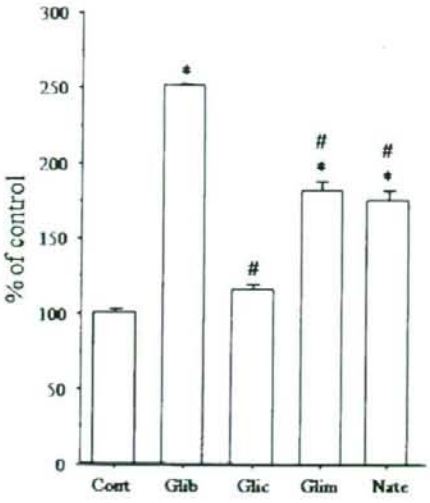

Fig. 3. Comparison of the stimulatory effects on ROS production with sulfonylureas and nateglinide. Data are expressed as mean percentage of control ± SEM (n = 10). *$P < .01$ vs nontreated cells (control). #$P < .01$ vs glibenclamide-treated cells. Glib indicates glibenclamide; Glic, gliclazide; Glim, glimepiride; Nate, nateglinide.

Sulfonylureas block β-cell adenosine triphosphate–sensitive K^+ channels, which leads to membrane depolarization, opening of voltage-dependent Ca^{2+} channels, Ca^{2+} influx, and elevated cytosolic Ca^{2+} concentration, and consequently induces insulin secretion. Several reports have suggested that sustained enhancement of Ca^{2+} influx caused by glibenclamide or tolbutamide induces apoptotic cell death in a β-cell line or islets [12,13]. In contrast, increased oxidative stress has been implicated as a potential mechanism for glucose toxicity on β-cells. Persistent exposure of β-cells to elevated glucose and ROS levels was reported to cause loss of transcription factors PDX-1 and MafA, which are essential to maintain normal levels of insulin promoter activity. Thus, the loss of PDX-1 and MafA leads to diminished insulin secretion [5]. Furthermore, several reports have shown that persistent exposure of β-cells to elevated glucose induces β-cell apoptosis, which was also mediated by excessive ROS production [6,7]. In addition, treatment with several antioxidants or antioxidant enzyme overexpression by gene transfer method was reported to protect from β-cell damage in animal models of type 2 diabetes mellitus [8,9,16]. Together, these findings suggest that oxidative stress may play an important role in the progressive deterioration of β-cell function and apoptosis. We recently reported that glibenclamide stimulated ROS production in the pancreatic β-cell cell line MIN6 [14], suggesting that increased ROS production may be a causative mechanism for glibenclamide-induced β-cell damage. In the present study, we further revealed that another sulfonylurea, glimepiride, and a new insulin secretagogue, nateglinide, also stimulated ROS production in MIN6 in a concentration-dependent manner from 0.1 to 10 μmol/L. The clinical relevance of these findings seems to be applicable because the concentrations used in the present study is within the therapeutic range. As for the source of ROS production, it has largely been established that the mitochondrial respiratory chain is an important site of ROS production within cells, including β-cells [17]. In contrast, NAD(P)H oxidase has received increasing attention as one of the most important source of

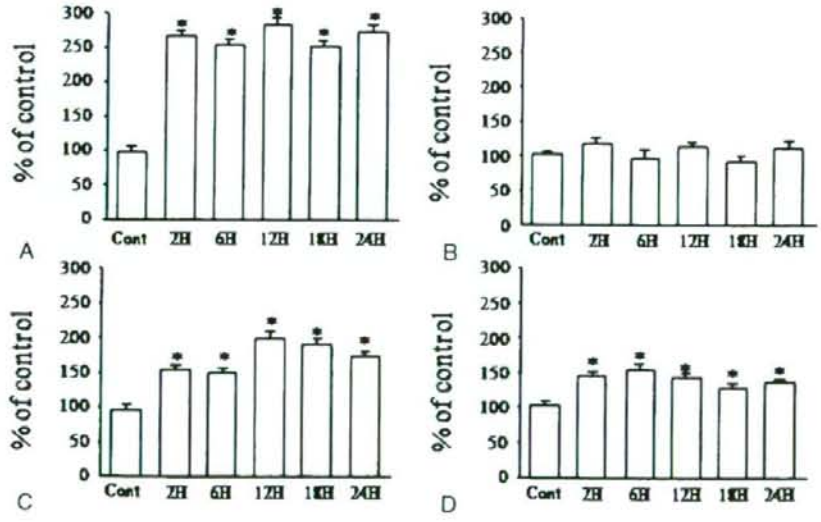

Fig. 4. Time course of ROS production by sulfonylureas and nateglinide. After incubation with sulfonylureas or nateglinide at a concentration of 10 μmol/L for 2, 6, 12, 18, or 24 hours, production of ROS was evaluated by DCF-DA method. Glibenclamide (n = 12) (A), gliclazide (n = 10) (B), glimepiride (n = 12) (C), and nateglinide (n = 10) (D). Data are expressed as mean percentage of control ± SEM. *$P < .01$ vs nontreated cells each (control).

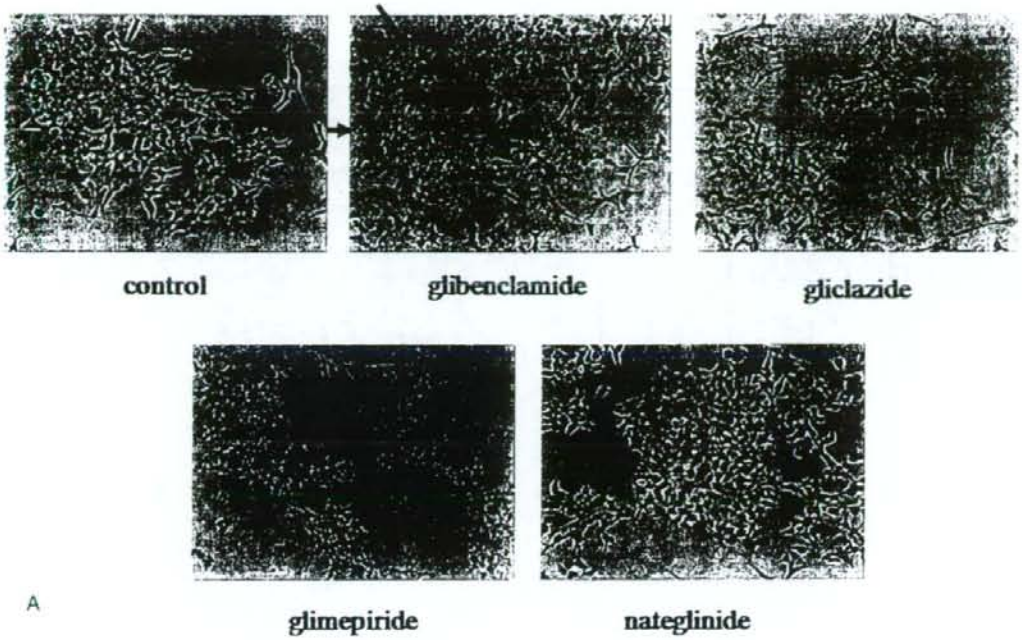

Fig. 5. Effect of sulfonylureas and nateglinide on apoptosis in MIN6 cells. The MIN6 cells were incubated with test media containing 1% FBS and 5.5 mmol/L glucose with glibenclamide, gliclazide, glimepiride, and nateglinide at a concentration of 10 μmol/L. After 48 hours of incubation, apoptosis was evaluated by TUNEL assay. A, Representative images of apoptotic cells. Arrows indicate brown-colored TUNEL-positive cells. B, Quantitative analysis of the rates of apoptotic cells induced by sulfonylureas and nateglinide. Data are expressed as mean percentage of control ± SEM (n = 4). $^{*}P < .01$ vs control. $^{\#}P < .01$ vs glibenclamide-treated MIN6 cells.

ROS production in vascular cells [18]. Previously, we and other investigators have shown that elevated glucose levels stimulate ROS production via PKC-dependent activation of NAD(P)H oxidase [19-21]. Recently, several reports have shown the presence of NAD(P)H oxidase in pancreatic β-cell [22,23]. In the present results, the stimulatory effects on ROS production induced by sulfonylureas and nateglinide were completely blocked by treatment with a PKC inhibitor and NAD(P)H oxidase inhibitors, but not significantly affected by treatment with other inhibitors of flavoproteins such as mitochondria electron transport chain (rotenone), xanthine oxidase (oxypurinol), or nitric oxide synthase (*N*-methyl-L-

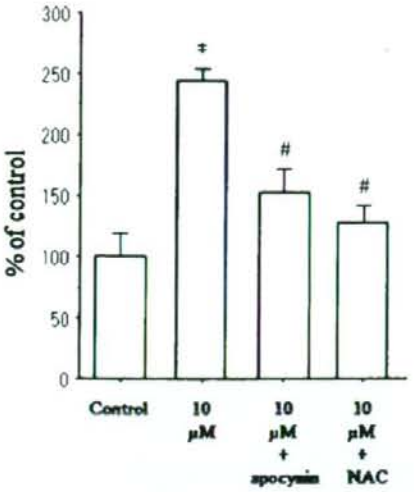

Fig. 6. Effect of apocynin and NAC on the rates of apoptotic cells induced by glibenclamide. The MIN6 cells were exposed to glibenclamide with or without apocynin or NAC. Data are expressed as mean percentage of control ± SEM (n = 6). *$P < .01$ vs control. #$P < .01$ vs glibenclamide-treated MIN6 cells.

arginine). Thus, these findings suggest that the stimulatory effects on ROS production induced by sulfonylureas and nateglinide may be mediated by a PKC-dependent activation of NAD(P)H oxidase. The present study also revealed that these agents further increased the numbers of apoptotic β-cells, but this was significantly blocked by the treatment with NAD(P)H oxidase inhibitors or antioxidant NAC. These results suggest that these agents might induce β-cell apoptosis via NAD(P)H oxidase–dependent ROS production.

Of great interest, in contrast with other sulfonylureas and nateglinide, gliclazide did not significantly stimulate ROS production. These findings may be consistent with one previous report showing that gliclazide attenuated apoptotic β-cell death induced by hydroxyl peroxide treatment [24]. Gliclazide may also possess radical scavenging properties including inhibition of low-density lipoprotein oxidation [25], inhibition of *o*-dianisidine photooxidation [26], and reduction of lipid peroxides [27]. Furthermore, a recent report has confirmed its scavenging activity against hydroxyl and superoxide radicals using an electron spin resonance method [28]. Therefore, it is likely that gliclazide might stimulate ROS production in β-cells via the same mechanism as other sulfonylureas, but at the same time diminishes oxidative stress via its radical scavenging effect. In parallel with the results of ROS production, gliclazide did not significantly induce the increased rates of β-cell apoptosis. Thus, gliclazide may be more protective against β-cell damage than other sulfonylureas or nateglinide. In support of this concept, a recent retrospective analysis showed that patients treated with gliclazide needed to administer insulin less frequently than glibenclamide, suggesting that gliclazide is less likely to induce β-cell failure compared with glibenclamide [29]. However, there are very few clinical studies showing the reduced frequencies of β-cell failure of gliclazide as compared with those clinical studies related to glimepiride or nateglinide. The short-acting insulin secretagogue nateglinide has a distinct action from sulfonylureas in vivo, with rapid elimination from the body and a plasma half-life of less than 2 hours. Therefore, it is predictable that the stimulatory effect of nateglinide on ROS produc-

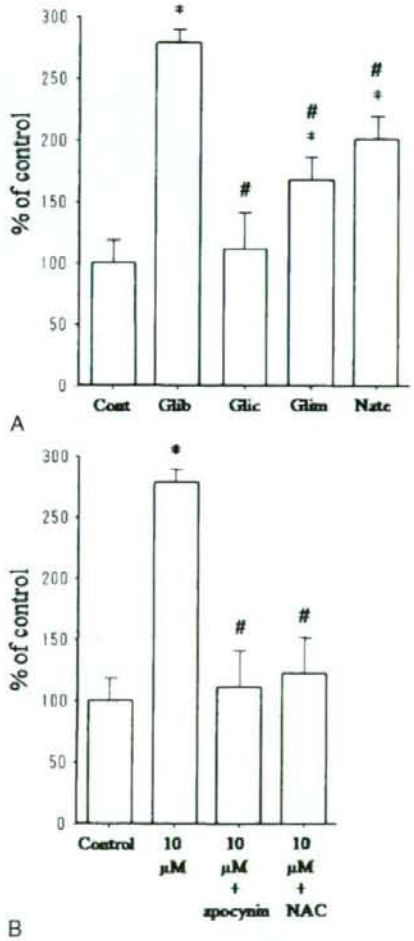

Fig. 7. Effect of sulfonylureas and nateglinide on apoptosis and effect of apocynin and NAC on the rates of apoptotic cells induced by glibenclamide in pancreatic islets. Islet cells were incubated with glibenclamide, gliclazide, glimepiride, and nateglinide at a concentration of 10 μmol/L. After 48 hours of incubation, apoptosis was evaluated by TUNEL assay. A, Quantitative analysis of the rates of apoptotic cells induced by sulfonylureas and nateglinide. B, Effect of apocynin and NAC for the rates of apoptotic cells induced by glibenclamide. The islet cells were exposed to glibenclamide with or without apocynin or NAC. Data are expressed as mean percentage of control < .01 vs control. #$P < .01$ vs glibenclamide-treated islet cells.

Optimal Cut Points of Waist Circumference for the Clinical Diagnosis of Metabolic Syndrome in the Japanese Population

YUKA MATOBA, MD[1]
TOYOSHI INOGUCHI, MD, PHD[1]
SHIGERU NASU, MD[2]
SHIZU SUZUKI, MD[2]
TOSHIHIKO YANASE, MD, PHD[1]
HAJIME NAWATA, MD, PHD[3]
RYOICHI TAKAYANAGI, MD, PHD[1]

In 2005, the International Diabetes Federation (IDF) and the Japanese Committee for the Diagnostic Criteria of Metabolic Syndrome (Japanese definition) proposed metabolic syndrome definitions for the Japanese population (1,2). Both definitions included waist circumference as an essential component and adopted cut points of 85 cm for men and 90 cm for women based on the relationship between waist circumference and visceral fat area by computed tomography (3). However, those cut points have been in dispute because of their suboptimal sensitivity and specificity (4–6). Recently, the IDF proposed common cut points for the whole Asian population including the Japanese: 90 cm for men and 80 cm for women (7). In this study, we investigated optimal waist cut points to identify subjects with multiple risk factors in the Japanese population and verified the cut points to predict carotid intima-media thickening in metabolic syndrome subjects as a surrogate marker of early atherosclerosis and cardiovascular disease (8–10).

RESEARCH DESIGN AND METHODS

We reviewed cross-sectional data from 1,658 men and 1,116 women (aged 48.8 ± 9.8 and 46.8 ± 10.4 years, respectively) who had annual medical checkup services provided by their employers. The medical checkup took place from May 2005 to November 2006 at the Human Dry Dock Center Wellness in Fukuoka, Japan. Subjects on antihypertensive and/or antidiabetic medications were included as individuals with hypertension and/or diabetes, respectively. We excluded 158 subjects on medications for dyslipidemia because we were unable to determine whether they were treated for hypercholesterolemia or hypertriglyceridemia. The study protocol was approved by the ethics committee of the related institutes.

Measurements

Waist circumference was measured at the level of the umbilicus. Blood pressure was measured at rest using an automatic sphygmomanometer. All blood samples were withdrawn after an overnight 10-h fast. Mean carotid intima-media thickness (IMT) was measured by ultrasonography (SDU-2200; Shimadzu, Kyoto, Japan) equipped with IMT measurement software (Intimascope; Media Cross, Tokyo, Japan) (8).

Definitions of metabolic syndrome

We diagnosed metabolic syndrome by each waist cut point and two or more of the following risk factors, using the IDF definition, 1) blood pressure, systolic ≥130 and/or diastolic ≥85 mmHg, 2) triglycerides ≥150 mg/dl, 3) HDL cholesterol <40 mg/dl in men and <50 mg/dl in women, and 4) fasting plasma glucose ≥100 mg/dl; and using the Japanese definition, 1) blood pressures, same as the IDF, 2) triglycerides ≥150 mg/dl and/or HDL cholesterol <40 mg/dl, and 3) fasting plasma glucose ≥110 mg/dl.

Statistical analyses

Receiver operating characteristic (ROC) curve analyses were performed using Dr. SPSS II 11.0.1J software (SPSS Japan, Tokyo, Japan), and the optimal cut points were obtained from the Youden index, maximum (sensitivity + specificity − 1) (11) (12). ANOVA and multiple comparisons were used to compare carotid IMT among subject groups for statistical significance and were performed using StatView software (SAS Institute, Cary, NC). Statistical significance was inferred at $P < 0.05$.

RESULTS

We plotted ROC curves to determine optimal waist cut points (87 cm in men and 80 cm in women) to identify subjects with multiple risk factors with maximum sensitivity and specificity using the Youden index for both of the definitions (Fig. 1*A–D*). Using the optimal cut point of 87 cm for men, the sensitivity and specificity were 68 and 62% for the IDF and 70 and 57% for the Japanese definition, whereas the cut point of 90 cm, compared with 87 cm, showed lower sensitivity of 51% for the IDF and 53% for the Japanese definition (Fig. 1*A* and *B*). Using the optimal cut point of 80 cm for women, the sensitivity and specificity were 74 and 70% for the IDF and 84 and 68% for the Japanese definition. The former IDF and Japanese cut point of 90 cm showed inadequate sensitivity of 33% for the IDF and 38% for the Japanese definition (Fig. 1*C* and *D*).

Next, we divided the subjects into subgroups by waist circumference. In men, the cut points of 85, 87, and 90 cm identified 25.0, 21.9, and 16.2% of subjects with the metabolic syndrome, respectively, for the IDF definition and 14.9, 13.4, and 10.2%, respectively, for the Japanese definition. In subgroups with abdominal adiposity, IMT increased significantly in metabolic syndrome sub-

From the [1]Department of Medicine and Bioregulatory Science, Graduate School of Medical Sciences, Kyushu University, Fukuoka, Japan; [2]Human Dry Dock Center Wellness, Fukuoka, Japan; and [3]Fukuoka Prefectural University, Fukuoka, Japan.

Address correspondence and reprint requests to Yuka Matoba, MD, Department of Medicine and Bioregulatory Science, Kyushu University, 3-1-1 Maidashi, Higashi-ku, Fukuoka 812-8582, Japan. E-mail: ymatoba@intmed3.med.kyushu-u.ac.jp.

Received for publication 25 April 2007 and accepted in revised form 29 November 2007.

Published ahead of print at http://care.diabetesjournals.org on 10 December 2007. DOI: 10.2337/dc07-0802.

Abbreviations: IDF, International Diabetes Federation; IMT, intima-media thickness; ROC, receiver operating characteristic.

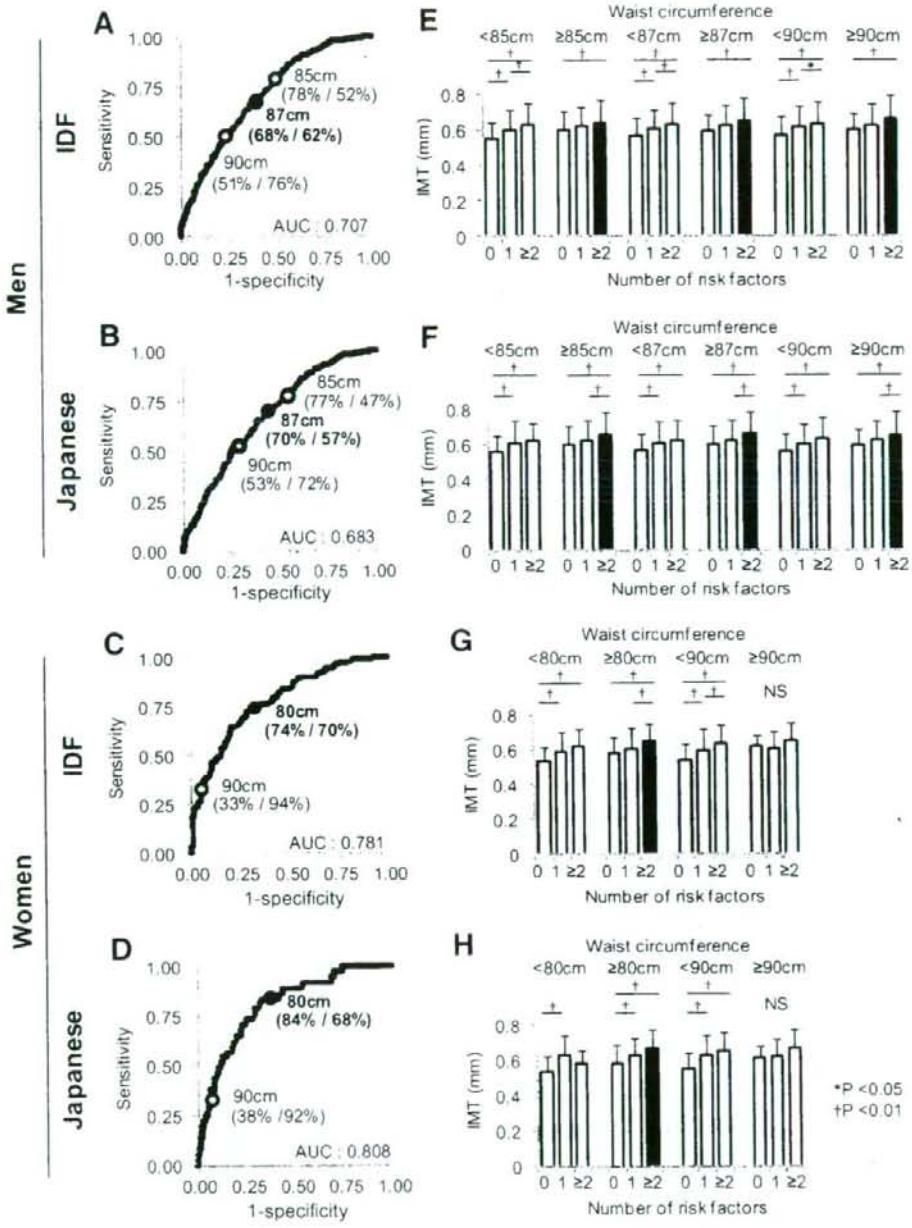

Figure 1—*ROC curves for waist circumference and intima-media thickening in metabolic syndrome subjects. ROC curves for waist circumference were plotted (A–D). ●, optimal cutpoint with maximum sensitivity and specificity determined using the Youden Index. ○, cut point of the conventional and revised waist cut points. The numbers in parentheses under the waist circumference indicate sensitivity (%)/specificity (%) at each cut point. AUC, area under the curve. Mean IMT were obtained in subgroups using the optimal or conventional or revised waist cut points and the IDF or the Japanese definition (E–H). In subgroups with abdominal adiposity, black bars indicate the metabolic syndrome subjects with significantly increased IMT.*

jects with multiple risk factors, suggesting feasibility of the cut points of 85, 87, and 90 cm (Fig. 1*E* and *F*). With any of the above cut points, the increasing IMT in metabolic syndrome subjects was more specific using the Japanese definition (Fig. 1*E* and *F*).

In women, the cut points of 80 and 90 cm identified 7.0 and 3.0% of metabolic syndrome subjects, respectively, for the IDF definition and 2.8 and 1.3% of subjects, respectively, for the Japanese defini-

tion. In subjects with waist circumference ≥90 cm, there was no significant difference in IMT using either definition. In contrast, when we used the cut point of 80 cm, the IMT increased significantly in metabolic syndrome subjects (Fig. 1*G* and *H*), suggesting the feasibility of the optimal cut points (80 cm) and the revised IDF definition. The increasing IMT in metabolic syndrome subjects was more specific using the IDF definition (Fig. 1*G* and *H*).

The optimal cut points obtained in the present study, 87 cm for men and 80 cm for women, predicted increasing IMT in metabolic syndrome subjects. These cut points were equivalent to those in a previous report by Hara et al. (4) that proposed ~85 cm for men and ~80 cm for women.

Finally, a potential limitation of this study is that the subjects were exclusively company employees who may not represent the whole Japanese population. Another metabolic syndrome definition, which includes waist criteria as an optional component, was proposed by the American Heart Association/National Heart, Lung and Blood Institute (13). Including requisiteness of waist circumference, further studies are required to optimize metabolic syndrome definitions in larger populations.

CONCLUSIONS— The optimal waist cut points were 87 cm for men and 80 cm for women. These cut points not only had maximum sensitivity and specificity to identify subjects with multiple risk factors but also predicted increased IMT in metabolic syndrome subjects. In men, both definitions were feasible. However, the Japanese definition (85 cm) surpasses the IDF definition (90 cm), since the cut point of 90 cm decreased sensitivity. In women, only the IDF definition (80 cm) was feasible to identify metabolic syndrome subjects in Japanese population.

References

1. Zimmet P, Magliano D, Matsuzawa Y, Alberti G, Shaw J. The metabolic syndrome: a global public health problem and a new definition. *J Atheroscler Thromb* 12:295–300, 2005
2. Metabolic syndrome: definition and diagnostic criteria in Japan. *J Jpn Soc Intern Med* 94:188–203, 2005
3. The Examination Committee of Criteria for 'Obesity Disease' in Japan; the Japan Society for the Study of Obesity. New criteria for 'obesity disease' in Japan. *Circ J* 66:987–992, 2002
4. Hara K, Matsushita Y, Horikoshi M, Yoshiike N, Yokoyama T, Tanaka H, Kadowaki T. A proposal for the cutoff point of waist circumference for the diagnosis of metabolic syndrome in the Japanese population. *Diabetes Care* 29:1123–1124, 2006
5. Miyawaki T, Hirata M, Moriyama K, Sasaki Y, Aono H, Saito N, Nakao K: Metabolic syndrome in Japanese diagnosed with visceral fat measurement by computed tomography. *Proc Japan Acad* 81:471–479, 2005
6. Hayashi T, Boyko EJ, McNeely MJ, Leonetti DL, Kahn SE, Fujimoto WY. Minimum waist and visceral fat values for identifying Japanese Americans at risk for the metabolic syndrome. *Diabetes Care* 30:120–127, 2007
7. The IDF consensus worldwide definition of the metabolic syndrome [article online], 2006. Available from http://www.idf.org/webdata/docs/MetS_def_update2006.pdf. Accessed 11 October 2007
8. Yanase T, Nasu S, Mukuta Y, Shimizu Y, Nishihara T, Okabe T, Nomura M, Inoguchi T, Nawata H. Evaluation of a new carotid intima-media thicknessn measurement by B-mode ultrasonography using an innovative measurement software, intimascope. *Am J Hypertens* 19:1206–1212, 2006
9. Dijk JM, van der Graaf Y, Bots ML, Grobbee DE, Algra A. Carotid intima-media thickness and the risk of new vascular events in patients with manifest atherosclerotic disease: the SMART study. *Eur Heart J* 27:1971–1978, 2006
10. Ludwig M, von Petzinger-Kruthoff A, von Buquoy M, Stumpe KO. [Intima media thickness of the carotid arteries: early pointer to arteriosclerosis and therapeutic endpoint]. *Ultraschall Med* 24:162–174, 2003 [article in German]
11. Youden WJ. Index for rating diagnostic tests. *Cancer* 3:32–35, 1950
12. Perkins NJ, Schisterman EF. The inconsistency of "optimal" cutpoints obtained using two criteria based on the receiver operating characteristic curve. *Am J Epidemiol* 163:670–675, 2006
13. Grundy SM, Cleeman JI, Daniels SR, Donato KA, Eckel RH, Franklin BA, Gordon DJ, Krauss RM, Savage PJ, Smith SC Jr, Spertus JA, Costa F. Diagnosis and management of the metabolic syndrome: an American Heart Association/National Heart, Lung, and Blood Institute Scientific Statement. *Circulation* 112:2735–2752, 2005

DIABETES RESEARCH AND CLINICAL PRACTICE 82 (2008) 378–382

available at www.sciencedirect.com

ScienceDirect

journal homepage: www.elsevier.com/locate/diabres

High prevalence of peripheral arterial disease diagnosed by low ankle–brachial index in Japanese patients with diabetes: The Kyushu Prevention Study for Atherosclerosis

Yasutaka Maeda [a], *Toyoshi Inoguchi* [a,*], *Hirotaka Tsubouchi* [a], *Fumi Sawada* [a], *Shuji Sasaki* [a], *Masakazu Fujii* [a], *Ryoko Saito* [a], *Toshihiko Yanase* [a], *Michio Shimabukuro* [c], *Hajime Nawata* [b], *Ryoichi Takayanagi* [a]

[a] *Department of Medicine and Bioregulatory Science, Graduate School of Medical Sciences, Kyushu University, 3-1-1 Maidashi, Higashi-ku, Fukuoka 812-8582, Japan*

[b] *Graduate School of Medical Sciences, Kyushu University, 3-1-1 Maidashi, Higashi-ku, Fukuoka 812-8582, Japan*

[c] *Second Department of Internal Medicine, Faculty of Medicine, University of the Ryukyus, 1 Senbaru, Nishihara, Okinawa 903-0213, Japan*

ARTICLE INFO

Article history:
Received 11 December 2007
Received in revised form
4 July 2008
Accepted 1 September 2008
Published on line 19 October 2008

Keywords:
Ankle–brachial index (ABI)
Peripheral arterial disease (PAD)
Arteriosclerosis obliterans (ASO)
Type 2 diabetes

ABSTRACT

We examined the prevalence of peripheral arterial disease (PAD) in Japanese diabetic patients with ankle–brachial index (ABI). Outpatients with diabetes ($n = 4249$) who were regularly visiting Kyushu University Hospital, its 17 related hospitals, Ryukyu University Hospital and its 6 related hospitals were enrolled in the Kyushu Prevention Study for Atherosclerosis from 2001 to 2003. At baseline, ABI was measured using a device "form PWV/ABI". Valid information was available for 3906 diabetic patients (mean age: 60.8 years) including 1612 elderly patients (>65 years). Patients with a low ABI (≤0.9) on either side or on both sides were considered to have PAD. The prevalence of PAD patients with ABI ≤ 0.9 was 7.6% in all diabetic subjects. Elderly patients (>65 years) had a higher prevalence of PAD (12.7%) compared with younger patients (≤65 years) (4.0%). In addition, the rate of patients who had been diagnosed accurately as having PAD before enrollment was low (24.4%). The prevalence of PAD was high in Japanese patients with diabetes, especially in elderly patients, in contrast to low rates of accurate diagnosis. Better diagnostic efforts and more intensive treatments are needed to improve quality of life and the overall prognosis of life in Japanese diabetic patients.

1. Introduction

Peripheral arterial disease (PAD) is more frequent in diabetic patients compared with non-diabetic subjects. Limb amputation is a frequent clinical complication of PAD and is common in patients with diabetes. In addition, recent studies have shown that PAD is associated with a significantly elevated risk of morbidity and mortality due to cardiovascular diseases [1–3]. A recent study that examined ethnic differences in PAD showed that the prevalence of PAD in Asians was significantly lower than that of non-Hispanic whites, blacks and Hispanics [4]. However, there have been very few studies examining the

* *Corresponding author.* Tel.: +81 92 642 5284; fax: +81 92 642 5287.
E-mail address: toyoshi@intmed3.med.kyushu-u.ac.jp (T. Inoguchi).
0168-8227/$ – see front matter © 2008 Elsevier Ireland Ltd. All rights reserved.
doi:10.1016/j.diabres.2008.09.008

prevalence of PAD of diabetic patients based on large-scale populations in Asia, especially in Japan. Although one report showed a low prevalence of PAD (1.9%) in Japanese diabetic patients in 1983, early studies, including this study, generally relied on absent foot pulses or the presence of claudication to identify individuals with PAD [5]. Recently, the role of ankle-brachial index (ABI) in the detection of PAD has been well established. In addition, a new device that can simultaneously measure blood pressures in the arms and legs and automatically calculate ABI has been developed. Therefore, in the present study, we estimated the prevalence of PAD in 3906 Japanese patients with diabetes by ABI measurement using such a device. In addition, since there is some evidence for the underdiagnosis of PAD, we also examined the prevalence of PAD in patients who had been accurately diagnosed as having PAD before the measurement of ABI in this study.

2. Materials and methods

2.1. Subjects

This study was based on data from the Kyushu Prevention Study for Atherosclerosis, an ongoing prospective multicenter survey. Outpatients with diabetes ($n = 4249$) who were regularly visiting Kyushu University Hospital, its 17 related hospitals, and Ryukyu University Hospital and its 6 related hospitals, were enrolled from 2001 to 2003 in this survey. Measurement of height, weight, systolic and diastolic blood pressure, 12-lead electrocardiography, eye fundus examination, and laboratory tests of blood and urine were carried out at baseline. Medical records included a history of cardiovascular events, current treatment for diabetes, and the use of other medications (including blood pressure-lowering drugs, lipid-lowering drugs, anti-thrombotic drugs). The participants provided informed consent and this study was approved by the ethics committees of the related institutes.

2.2. Clinical assessment

At baseline, a device "form PWV/ABI" (Omron Colin Co., Ltd., Komaki, Japan) was used to measure systolic blood pressure in the arms and legs of each subjects, and ABI was automatically calculated by the device as the ratio of systolic blood pressure in the leg to that in the arm on each side. Valid information was available for 3906 diabetic patients (mean age: 60.8 years) including 1612 elderly patients (≥65 years). According to the American Diabetes Association's criteria for PAD complicated with diabetic patients, PAD was defined as lower ABI < 0.9 and patients were classified as follows: lower ABI < 0.40 (severe), 0.40–0.69 (moderate), 0.70–0.89 (mild) and higher ABI > 1.30 (suspected poorly compressible arteries at the ankle level).

Retinopathy was assessed by a fundus examination by independent opthalmologists. Clinical proteinuria was defined as a level of + or more using the Albustix method. Coronary artery disease (CAD) was defined as a history of acute myocardial infarction, angina pectoris confirmed by a clinically significant obstruction on coronary angiography, or revascularization with angioplasty or coronary artery bypass. Cerebrovascular disease (CVD) was defined as a history of symptomatic stroke, confirmed by brain computed tomography or magnetic resonance imaging. Diabetic neuropathy was diagnosed from typical symptoms and physical findings examined by diabetologists. Hypertension was defined as systolic blood pressure ≥140 mm Hg or diastolic blood pressure ≥90 mm Hg, or the current use of any antihypertensive medication. Hyperlipidemia was determined by the previous history of such, or when the total cholesterol was >220 mg/dl and/or triglyceride >150 mg/dl. Smoking habit was defined as current smoking obtained by interview.

2.3. Statistical analysis

Continuous variables are presented as means ± S.D. and discrete variables are expressed as frequencies and percentages. Analyses were performed with StatView Version 5.0 software (SAS Institute Inc., Cary, NC, USA). For categorical variables, differences between patients were tested using the chi-square test with Yate's correction followed by Fisher's exact test. Adjusted odds ratios (OR) and their 95% confidence intervals (CI) were estimated with logistic regression models in order to investigate independent association between risk factors (age, sex, BMI, smoking, HbA1c, hypertension, hyperlipidemia, coronary artery disease, cerebrovascular atherosclerosis, diabetic neuropathy, diabetic retinopathy, diabetic nephropathy) and PAD.

3. Results

3.1. Clinical characteristics

Table 1 describes the demographic and clinical characteristics of the participants. The 3906 subjects with diabetes (mean age: 60.8 years) from the Kyushu Prevention Study for Atherosclerosis included 1612 elderly patients over 65 years (mean age: 71.8 years).

3.2. Prevalence of PAD

The prevalence of PAD with ABI < 0.9 was 7.6% in all diabetic subjects as shown in Table 2: ABI < 0.4; 0.2%, 0.4 ≤ ABI < 0.7; 2.3%, 0.7 ≤ ABI < 0.9; 5.2%. There was no significant difference in the prevalence of PAD between male and female (7.3 vs 8.1%). Elderly patients (≥65 years) had a much higher prevalence PAD than younger patients (<65 years) (12.7 vs 4.0%, $P < 0.01$). A high ABI (ABI ≥ 1.4) was found in 0.6% in all diabetic patients and in 0.9% in elderly patients.

3.3. Rates of diagnosis and treatment before ABI measurement

Accurate diagnosis rates of PAD before ABI measurement were quite low (24.4%) in subjects with a low ABI (<0.9), ABI < 0.4, 50.0%; 0.4 ≤ ABI < 0.7, 35.6%; 0.7 ≤ ABI < 0.9, 18.3%. Treatment rates of subjects with low ABI (<0.9) with anti-thrombotic agents or platelet inhibitor regardless of reasons to treat any atherosclerotic diseases including PAD, CAD and CVA were also low (45.1%) (data not shown) (Table 3).

Table 1 – Characteristics of all patients and elderly patients.

	All patients			Elderly patients (Age ≥ 65)		
	n = 3906	Male, n = 2317	Female, n = 1589	n = 1612	Male, n = 844	Female, n = 768
ABI	1.07 ± 0.13	1.09 ± 0.10	1.06 ± 0.13	1.05 ± 0.15	1.10 ± 0.20	1.00 ± 0.10
Age (years)	60.8 ± 11.9	59.4 ± 11.6	62.9 ± 12.0	71.8 ± 5.4	71.1 ± 5.0	72.5 ± 5.7
BMI (kg/m^2)	24.6 ± 4.1	24.4 ± 3.9	24.9 ± 4.3	23.9 ± 3.5	23.4 ± 3.1	24.4 ± 3.9
Smoking (%)	23.0	32.2	9.6	14.9	23.5	5.5
HbA1c (%)	7.8 ± 2.1	7.8 ± 2.2	7.8 ± 2.1	7.7 ± 1.9	7.6 ± 2.0	7.7 ± 1.9
Hypertension (%)	51.5	49.4	54.9	61.4	59.8	63.5
Hyperlipidemia (%)	46.9	41.1	55.5	49.4	40.9	59.2
Coronary artery disease (%)	14.9	15.0	14.8	23.4	24.5	22.4
Cerebrovascular atherosclerosis (%)	9.0	8.5	9.7	13.3	13.3	13.3
Diabetic neuropathy (%)	26.4	26.1	26.7	32.6	33.2	32.0
Diabetic retinopathy (%)	27.6	26.2	29.6	31.6	31.2	32.2
Proteinuria (%)	19.1	20.5	17.0	22.9	20.5	19.2

Data are means ± S.D. or percentages.

Table 2 – Prevalence of PAD diagnosed according to low ABI (<0.9) and distribution of ABI, compared by gender and age.

Classification by ABI	All patients	Gender		Age	
	n = 3906	Male, n = 2317	Female, n = 1589	<65, n = 2294	≥65, n = 1312
ABI < 0.9	296 (7.6)	168 (7.3)	128 (8.1)	91 (4.0)	205 (12.7)[b]
ABI < 0.4	6 (0.2)	2 (0.1)	4 (0.3)	2 (0.1)	4 (0.2)
0.4 ≤ ABI < 0.7	88 (2.3)	54 (2.3)	34 (2.1)	22 (1.0)	66 (4.1)[b]
0.7 ≤ ABI < 0.9	202 (5.2)	112 (4.8)	90 (5.7)	67 (2.9)	135 (8.4)[b]
0.9 ≤ ABI < 1.0	348 (8.9)	187 (8.1)	161 (10.1)[a]	176 (7.7)	172 (10.7)[b]
1.0 ≤ ABI < 1.3	3105 (79.5)	1848 (79.8)	1257 (79.1)	1925 (83.9)	1180 (73.2)[b]
1.3 ≤ ABI	166 (4.2)	120 (5.2)	46 (2.9)	106 (2.7)	60 (3.7)

Data are number (%).
[a] $P < 0.05$ vs male.
[b] $P < 0.01$ vs age < 65.

3.4. *Major risk factors for low ABI*

In our logistic regression model of all subjects, statistically significant risk factors for low ABI were age (OR: 1.64, 95% CI: 1.44, 1.87 for each 10 years increase), hypertension (OR: 1.57, 95% CI: 1.16–2.14), history of CAD (OR: 2.59, 95% CI: 1.91, 3.51), diabetic neuropathy (OR: 1.84, 95% CI: 1.37, 2.48), diabetic nephropathy (OR: 2.02, 95% CI: 1.49, 2.73). In contrast, elderly subjects (age ≥ 65) had the following risk factors for a low ABI: age (OR: 1.97, 95% CI: 1.45, 2.67 for each 10 years increase), hypertension (OR: 1.93, 95% CI: 1.28, 2.92), history of CAD (OR: 2.30, 95% CI: 1.60, 3.30), history of CVA (OR: 1.63, 95% CI: 1.06, 2.50), diabetic nephropathy (OR: 2.03, 95% CI: 1.40, 2.93) (Table 4).

Table 3 – Diagnosis rates of PAD before ABI measurement.

Classification by ABI	All patients n = 3906	Elderly patients age ≥ 65 n = 1612
ABI < 0.9	72/296 (24.4)	53/205 (25.9)
ABI < 0.4	3/6 (50.0)	3/4 (75.0)
0.4 ≤ ABI < 0.7	32/88 (36.4)	24/66 (36.4)
0.7 ≤ ABI < 0.9	37/202 (18.3)	26/135 (19.3)

Data are number (%). Diagnosis rate: proportion of patients who were diagnosed as having PAD before the measurement of ABI.

4. Discussion

In this large-scale, cross-sectional study, 7.6% of the diabetic patients had an ABI below 0.9, indicating the presence of PAD. In particular, elderly patients (≥65 years) had a higher prevalence of PAD (12.7%) compared with younger patients (<65 years) (4.0%). These values are much higher than those reported in 1983, where the prevalence of PAD was 1.9% in Japanese diabetic patients [5]. The difference between the two studies may reflect the increasing prevalence of PAD of Japanese diabetic patients due to changes of lifestyle such as eating habits and the decrease in physical activity in recent years. It may also be explained by the difference in the diagnosis method. Early studies generally relied on absent foot pulses or the presence of claudication to identify individuals with PAD. Recently, the role of ABI in the detection of PAD has been well established. Previous reports showed that the detection of PAD with at least

Table 4 – Risk factors for PAD (ABI < 0.9) in all patients and elderly patients.

Risk factors	All patients		Age ≥ 65	
	OR (95% CI)	P-value	OR (95% CI)	P-value
Age (for each 10 years increase)	1.51 (1.31, 1.74)	<0.0001	2.01 (1.48, 2.73)	<0.0001
Gender/Male	1.00 (0.75, 1.34)	0.9934	1.21 (0.84, 1.75)	0.3056
BMI (for each 1 kg/m^2 increase)	1.00 (0.96, 1.03)	0.8090	0.97 (0.92, 1.02)	0.2904
Smoking (%)	1.04 (0.73, 1.50)	0.8259	0.97 (0.58, 1.63)	0.9081
HbA1c (for each 1% increase)	0.99 (0.92, 1.06)	0.6626	0.91 (0.82, 1.00)	0.0607
Hypertension	1.50 (1.10, 2.03)	0.0097	1.95 (1.29, 2.95)	0.0014
Hyperlipidemia	0.97 (0.73, 1.29)	0.8369	0.90 (0.63, 1.29)	0.5554
Coronary artery disease	2.41 (1.78, 3.26)	<0.0001	2.34 (1.63, 3.35)	<0.0001
Cerebrovascular atherosclerosis	1.37 (0.94, 2.00)	0.0971	1.52 (0.98, 2.34)	0.0599
Diabetic neuropathy	1.85 (1.39, 2.47)	<0.0001	1.55 (1.09, 2.22)	0.0160
Diabetic retinopathy	1.09 (0.80, 1.48)	0.5960	1.32 (0.90, 1.93)	0.1590
Proteinuria	2.31 (1.69, 3.18)	<0.0001	2.11 (1.40, 3.17)	0.0004

Adjusted odds ratios (OR) of PAD with low ABI (<0.9) and 95% confidence intervals (CI) were calculated using logistic regression.

50% stenosis of lower extremity arteries had a 90% sensitivity and a 95% specificity when PAD was defined as an ABI below 0.9 [6–9]. In addition, a new device that enables simultaneous measurement of blood pressures in all four limbs has been developed. This device can automatically calculate ABI and reproducible results can be obtained regardless of the operator's technique. In this study, we used this device to measure ABI. A recent report showed that the prevalence of PAD was 2.7% in Japanese general population, and 3.4% in elderly subjects (≥65 years) as estimated by the same criteria using the same device [10]. Compared with the present results, these results suggest that the prevalence of PAD is approximately 3-fold higher in Japanese diabetic patients, and approximately 4-fold higher in elderly diabetic patients than in the general Japanese population.

Previous reports indicated that clinical symptoms reported by patients or an absent pulse diagnosed by physicians were inadequate for reliable screening of early PAD [7,11–13]. Therefore, screening for PAD using ABI is recommended in diabetes. Nevertheless, this recommendation has not been universally embraced. Several reports have shown that PAD is still underdiagnosed and risk factor management may be suboptimal. The present study showed that the rates of patients who had been diagnosed accurately as having PAD before the measurement of ABI in this study were quite low (24.4%), indicating that the underdiagnosis of PAD in the present study is worse than previously reported. This is because clinicians may underestimate the prevalence of PAD in Japanese diabetic patients. Many studies have shown that PAD with a low ABI was associated with cardiovascular [14] and all-cause mortality [15–18]. The accurate detection of PAD with ABI measurement and intensive treatment could improve the overall prognosis as well as activity in daily life and quality of life in Japanese diabetic patients.

In the present study, we found the proportion of diabetic patients with a high ABI (≥1.3) was not low (4.2%). Because previous reports have shown that a high ABI predicts cardiovascular and all-cause mortality with similar strength as ABI < 0.9 [18], clinicians should still pay attention to a high ABI. It should be noted that a borderline low ABI (0.9–1.0) is also reported to have a greater risk of cardiovascular and all-cause mortality than normal ABI (1.0–1.4). The present study showed a high prevalence (5.2% in all subjects and 8.4% in elderly subjects) of this range of ABI in Japanese diabetic patients. Future prospective studies are needed to determine whether this range of ABI is associated with cardiovascular and all-cause mortality in Japanese diabetic patients.

The predisposing factors for PAD, estimated with a multiple logistic regression model, were similar to the results of previous studies examining other atherosclerotic diseases. Age, hypertension, coronary artery disease and proteinuria were strongly associated with PAD. While one study has reported that males were at greater risk for PAD [19], we found no significant differences in the prevalence of PAD between males and females in accordance with some studies in diabetic subjects [20]. Smoking is one of the highest risk factors for vascular atherosclerosis, including PAD [14,21]. However, in our study, a history of smoking was not significantly associated with PAD, probably because our definition of smoking history did not include ex-smoker. In addition, there was no significant correlation between PAD and either HbA1c or hyperlipidemia. These results may be due to the limited assessment in this cross-sectional study.

In conclusion, Japanese patients with diabetes had a high prevalence of PAD in contrast to low rate of diagnosis, especially in elderly subjects. Increasing diagnostic efforts and intensive treatments are needed to improve quality of life and the life prognosis in Japanese diabetic patients.

Acknowledgements

We thank other members of the Kyushu Prevention Study for Atherosclerosis Investigators, Dr. F. Umeda, Dr. K. Mimura, Dr. Y. Tajiri, Fukuoka City Medical Association Hospital, Dr. M. Matsumoto, Dr. H. Ishii, Dr. N. Ueno, Kitakyushu Municipal Medical Center, Dr. T. Yamauchi, Dr. J. Watanabe, Yukuhashi Central Hospital, Dr. S. Hiramatsu, Dr. J. Ogo, National Kyushu Medical Center, Dr. T. Okajima, Kokura National Hospital, Dr. T. Kimura, Social Insurance Nakabaru Hospital, Dr. Y. Sako, Dr. N. Sekiguchi, Saiseikai Fukuoka General Hospital, Dr. H. Katsuren, Heartlife Hospital, Dr. S. Natori, Dr. T. Kodera, Iizuka Hospital, Dr. M. Higa, Dr. T. Shimabukuro, Tomishiro Central Hospital, Dr. S. Nasu, Dr. S. Suzuki, Wellness Clinic, Dr.